

DOI: 10.1002/chem.201600897

## Linear Optical and Third-Order Nonlinear Optical Properties of Some Fluorenyl- and Triarylamine-Containing Tetracyanobutadiene Derivatives

Ziemowit Pokladek,<sup>[a]</sup> Dr. Nicolas Ripoche,<sup>[b,c]</sup> Dr. Marie Betou,<sup>[d]</sup> Dr. Yann Trolez,<sup>\*,[d]</sup> Dr. Olivier Mongin,<sup>[b]</sup> Dr. Joanna Olesiak-Banska,<sup>[a]</sup> Dr. Katarzyna Matczyszyn,<sup>\*,[a]</sup> Prof. Marek Samoc,<sup>[a]</sup> Prof. Mark G. Humphrey,<sup>[c]</sup> Dr. Mireille Blanchard-Desce,<sup>[e]</sup> and Dr. Frédéric Paul<sup>\*,[b]</sup>

**A glass of fluorescence!** Selected optical properties of four new tetracyanobutadiene derivatives incorporating fluorenyl and diphenylamino moieties have been studied (see figure). While nonluminescent in solution at ambient temperatures, these electroactive derivatives become luminescent in more rigid media. They are also two-photon absorbers in the near-IR range (800-1050 nm).

**Keywords:** Tetracyanobutadiene • Nonlinear Optical Properties • Two-photon Absorption • Luminescence • Alkyne

---

[a] Z. Pokladek, Dr J. Olesiak-Banska, Dr. K. Matczyszyn, Pr. M. Samoc  
Advanced Materials Engineering and Modeling Group  
Faculty of Chemistry  
Wroclaw University of Technology  
50-370 Wroclaw

[b] N. Ripoche, Dr. O. Mongin, Dr. F. Paul  
Institut des Sciences Chimiques de Rennes, CNRS (UMR 6226)  
Université de Rennes 1  
Campus de Beaulieu, 35042 Rennes Cedex (France)  
Tel: (+33) 02-23-23-59-62  
E-mail: frederic.paul@univ-rennes1.fr

[c] Pr. M. G. Humphrey  
Research School of Chemistry, Australian National University  
Canberra, ACT 2601 (Australia)

[d] Dr. M. Betou, Dr. Y. Trolez  
Ecole Nationale Supérieure de Chimie de Rennes,  
Institut des Sciences Chimiques de Rennes, CNRS (UMR 6226)  
11 allée de Beaulieu, CS 50837  
35708 Rennes Cedex 7 (France)

[e] Dr. M. Blanchard-Desce  
ISM, CNRS (UMR 5255)  
Université Bordeaux  
33400 Talence France

Supporting information for this article is given via a link at the end of the document.

## Linear Optical and Third-Order Nonlinear Optical Properties of Some Fluorenyl- and Triarylamine-Containing Tetracyanobutadiene Derivatives

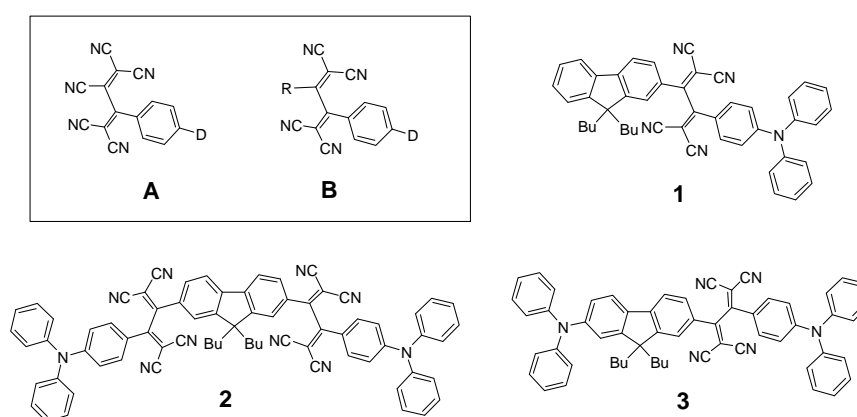
Ziemowit Pokladek,<sup>[a]</sup> Dr. Nicolas Ripoche,<sup>[b,c]</sup> Dr. Marie Betou,<sup>[d]</sup> Dr. Yann Trolez,<sup>\*,[d]</sup> Dr. Olivier Mongin,<sup>[b]</sup> Dr. Joanna Olesiak-Banska,<sup>[a]</sup> Dr. Katarzyna Matczyszyn,<sup>\*,[a]</sup> Prof. Marek Samoc,<sup>[a]</sup> Prof. Mark G. Humphrey,<sup>[c]</sup> Dr. Mireille Blanchard-Desce,<sup>[e]</sup> and Dr. Frédéric Paul<sup>\*,[b]</sup>

**Abstract.** The synthesis and characterization of four new tetracyanobutadiene (TCBD) derivatives (**1-3** and **2'**) incorporating 2- or 2,7-fluorenyl and diphenylamino moieties are reported. The electroactivity of **1-3** and **2'** was studied by cyclic voltammetry (CV), while the linear optical and (third-order) nonlinear optical (NLO) properties were investigated by electronic spectroscopy and Z-scan studies, respectively. All experimental investigations were rationalized by DFT computations, providing an insight into the electronic structure of these derivatives and on their application potential. We show that these derivatives are nonluminescent in solution at ambient temperatures, but become fluorescent in solvent glasses. This finding constitutes an unprecedented observation for TCBD derivatives. Also, we show by Z-scan studies that these derivatives behave as two-photon absorbers in the near-IR range (800-1050 nm). These third-order NLO properties are discussed and compared with those of their alkynyl precursors (**4-6**), which have been investigated by two-photon excited fluorescence (TPEF).

## Introduction

Tetracyanobutadienes (TCBDs) and, more generally, polycyanoethylenes are powerful acceptor groups,<sup>[1]</sup> which, when conjugated to donor groups through an unsaturated spacer such as in **A** (Scheme 1), give rise to donor-acceptor molecular structures possessing remarkable nonresonant quadratic<sup>[1], [2]</sup> and cubic<sup>[3]</sup> nonlinear optical (NLO) responses.<sup>[4]</sup>

Furthermore, in the latter case, the seminal investigations of the Diederich group have clearly shown that related derivatives such as **B** ( $R = C=C(4-C_6H_4NMe_2)$ ;  $D = NMe_2$ ) show outstanding promise in the field of integrated nonlinear optics, given that these structures possess a large, off-resonant cubic nonlinear molecular polarizability ( $\gamma_0$ ) and give rise to high-quality films by molecular beam deposition on glass supports.<sup>[5]</sup> These remarkable features can be attributed to the tetracyanobutadiene (TCBD) core that, while being thermally very stable and strongly electron-withdrawing, adopts a nonplanar conformation. It therefore limits any unwanted crystallization during the thermal deposition process, a very desirable property for the realization of optical devices such as waveguides.<sup>[6]</sup>



**Scheme 1.** Molecules targeted in this work and selected polycyanoethenylene derivatives (see inset).

However, apart from these promising results obtained with a handful of molecules, much remains to be learned about the third-order nonlinear optical properties of cyanoethenylene derivatives, in particular regarding their two-photon absorption (2PA) capabilities.<sup>[4]</sup> To the best of our knowledge, this particular cubic NLO property which is related to the imaginary part of  $\gamma$  has only been briefly examined,<sup>[7]</sup> and never with TCBD derivatives. Increasing our knowledge of 2PA cross-sections at specific wavelengths would strengthen interest in such molecules for integrated nonlinear optics by opening the possibility to use them in multiphoton optical gates<sup>[8]</sup> or in related devices for optical limiting or pulse

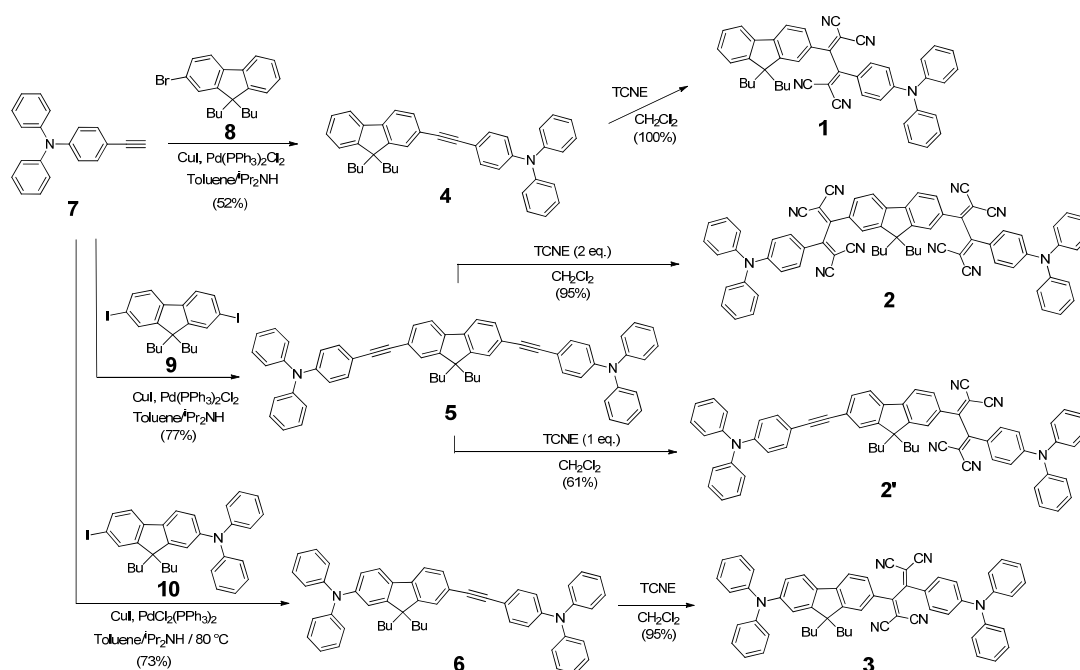
shaping.<sup>[7b]</sup> More generally, the lack of information about the 2PA capability of such stable, conjugated, and strongly polarized species is also unfortunate because multiphoton absorbers are key to many other important societal applications,<sup>[9]</sup> such as optical information storage, nanofabrication, photodynamic therapy, and, when fluorescent, molecular imaging.<sup>[7b]</sup>

With this in mind, an investigation into the 2PA properties of a series of TCBD derivatives (**1-3** in Scheme 1) incorporating fluorenyl and diphenylamino moieties was initiated, because these two building blocks are often constituents of good two-photon absorbers.<sup>[10]</sup> Furthermore, we were also wondering if the strongly fluorescent fluorenyl unit<sup>[11]</sup> could have any positive effect on the luminescence of the targeted compounds.<sup>[10f,12]</sup> Indeed, luminescence is a highly desirable feature for two-photon absorbers in biomedical applications.<sup>[7b,9a]</sup> However, the scant amount of data available in the literature about the luminescence of TCBD derivatives suggests that such species will, in general, be poor luminophores.<sup>[13]</sup> We thus report hereafter the synthesis<sup>[13]</sup> of **1-3** and the study of their linear optical and cubic nonlinear optical properties, with a particular emphasis on their 2PA capabilities. A comparison between **1** and **2** should evidence the influence of the (dipolar vs. symmetric and multipolar) molecular structure on these properties, while comparison between **1** and **3** should reveal the influence of a donor group appended to the 2- or 2,7-fluorenyl fragment.

## Results and Discussion

**Synthesis of the compounds.** The target compounds **1-3** were obtained from the corresponding alkyne derivatives **4-6** in one step by tetracyanoethylene (TCNE) cycloaddition at room temperature (Scheme 2).<sup>[4]</sup> Following the reaction of one equivalent of TCNE with **5**, the monoaddition adduct **2'** could be cleanly isolated in 61 % yield, while the double addition adduct **2** was isolated in 19 % yield in the same experiment. The required precursor alkynes **4-6** were themselves obtained by Sonogashira couplings from the known

starting compounds **7**,<sup>[14]</sup> **9**,<sup>[15]</sup> and **10**.<sup>[10c]</sup> The latter precursor was synthesized from **9** and diphenylamine in a similar fashion to the synthesis of its dodecyl analogue.<sup>[16]</sup> All the new compounds **1-6** and **10** were fully characterized and their structures were unambiguously established by mass spectrometry and by the combined use of NMR (for **1-3**, a combination of COSY and NOESY was used to assign all the observed protons) and IR/Raman spectroscopies, the latter techniques evincing the characteristic  $\nu_{C=C}$  modes expected for these molecules (Experimental Section and the Supporting Information).



**Scheme 2.** Synthesis of **1-3** and **2'**.

**Cyclic voltammetry.** The electrochemical properties of **1-3** (Table 1) were then investigated by cyclic voltammetry (CV) in dichloromethane (Figure 1). As expected from previous studies and also from DFT calculations (see later),<sup>[1b,c,4]</sup> all these new derivatives are electroactive, the tetracyanobutadiene moiety giving rise to two one-electron reductions located at each of the dicyanoethene moieties.<sup>[3c]</sup> Thus, **1**, **2'**, and **3** show a chemically reversible reduction process at around -0.4 V followed by a second process near -0.7 V versus SCE. The first reduction signal (around -0.4 V vs. SCE) of derivative **2**, featuring two TCBD

## Full Paper

units, is split into two distinct waves that are separated by approximately 77 mV, revealing the existence of electronic communication between the two TCBD units symmetrically disposed at either side of the 2,7-fluorenyl linker. Interestingly, this splitting is not observed for the second reduction process of these TCBD units. The latter takes place at the potential observed for **2'**, indicating that the two additional electrons injected into the LUMO of this compound do not interact, or at least not to the same extent as those associated with the first reduction process. In accordance with DFT calculations, this indicates that the C=C(CN)<sub>2</sub> subunits reduced first in **2** are most likely those located closer to the bridging ligand that may interact through its unsaturated  $\pi$  manifold, whereas the more remote 1,1-dicyanoethenyl units, closer to the electron-donating diphenylamino groups, are reduced in a subsequent and separate step at approximately 0.3 V more negative potentials. Based on the coincidence between the potential of the second reduction of **2** and those of **1**, **2'**, and **3**, a similar behavior certainly takes place with the other TCBD derivatives. The compounds **1-3** and **2'** also give rise to electrochemical events at higher potentials, closer to 1.0 V versus SCE. As suggested by the CVs of their precursor complexes (**4-6**) and DFT calculations, these pseudo reversible events (in the chemical sense) are not related to the presence of the TCBD units, but rather they correspond to the oxidation of the triaryl amino end groups. Indeed, such a process is known to occur around 0.9 V versus SCE,<sup>[17]</sup> as observed in the present case for **4-6**. In **1-3** and **2'**, these oxidations are shifted to more positive values (by ca. 0.3 V) because of the presence of the nearby TCBD electron-accepting groups, rendering this oxidation thermodynamically less favored. The first of these waves, observed at lowest potentials in **2'** and **3**, likely corresponds to the oxidation of the diphenylamino group most remote from the TCBD group, while the second wave, at higher potentials (around 1.3 V vs. SCE), corresponds to the oxidation of the diphenylamino group closer to the TCBD group. Besides being indicated by DFT calculations, this ordering is also supported by the good match between the potential of the second oxidation process in **2'** and that observed for **1**. Both processes are chemically irreversible at a scan rate of 0.1 V.s<sup>-1</sup>. For the symmetric derivative **2** and also for its symmetric precursor **5**, the oxidation of the two diphenylamino substituents takes place in an

apparent two-electron process, in line with a weak or nonexistent electronic coupling between these moieties across the central spacer. Based on the Rehm-Weller equation [Eq. (1)],<sup>[18]</sup> these data can be used to derive an estimate of the free enthalpy of formation of the intramolecular charge transfer (CT) state at lowest energy ( $\Delta G_{CT}$ ). The latter is given by the difference between the first amino-based oxidation potential and the first TCBD-based reduction potential in a given solvent (Table 1), corrected by an electrostatic term. Presently, estimates of the distances  $a$  in Equation (1) for **1-3** and **2'** could be obtained from molecular modelling studies (DFT) and the corresponding  $\Delta G_{CT}$  values were computed (Table 2).<sup>[19]</sup>

$$\Delta G_{CT} = E^\circ(D^+/D) - E^\circ(A/A^-) - \frac{e^2}{4\pi \epsilon_0 \epsilon a} \quad (1)$$

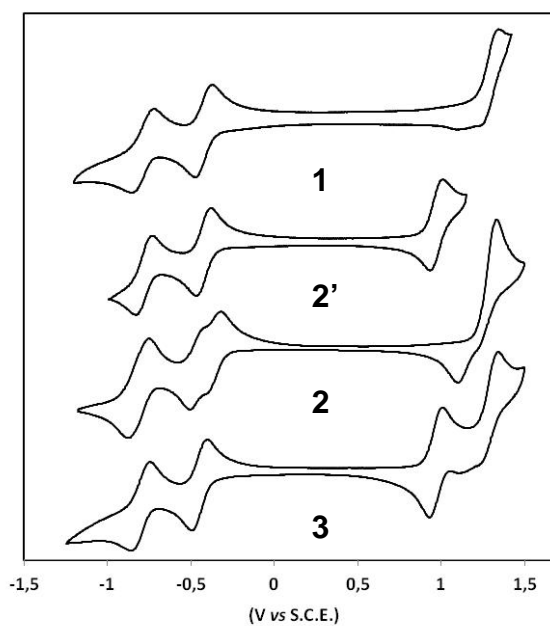


**Figure 1.** Cyclic voltammograms of **1-3** and **2'** in  $\text{CH}_2\text{Cl}_2/[n\text{-Bu}_4\text{N}][\text{PF}_6]$  (0.1 M) at 25 °C at 0.1 V/s.

**UV/Visible absorption.** The derivatives **1-3** and **2'** each exhibit a strong absorption extending beyond 700 nm in the visible range (Figure 2a) and giving them a dark-colored to fuchsia. According to DFT calculations (see below), these absorption bands correspond to several overlapped charge-transfer (CT) transitions from the electron-rich diphenylamino substituent(s) toward the electron-withdrawing TCBD/fluorenyl fragments (Table 2). Thus, the transitions at the lowest energy correspond to CT transition(s) from the occupied MOs located on the diphenylamino groups toward the TCBD  $\pi^*$  MOs. Their large  $\pi$ - $\pi^*$  character is supported by their overall weak (and somewhat erratic) solvatochromism (see the Supporting Information). Notably, their energy is always superior to the enthalpy of formation of the CT state ( $\Delta G_{CT}$ ) as derived by Equation (1). The next lowest-energy band(s) correspond to CT transition(s) toward the empty MOs on the fluorenyl/TCBD fragment. Finally, at higher energies,  $\pi^* \leftarrow \pi$  CT transitions toward the TCBDs but originating from the fluorenyl fragments are observed. This holds for both the dipolar and multipolar derivatives **1** and **2**, except that in the latter case, the donor groups are twice as numerous, resulting in a rough doubling in intensity of the low-energy transitions. The increased absorption at lowest energy for the dipolar compounds **3** and **2'** and the stronger absorption near 350 nm in the latter compound can be explained by the presence of CT transitions taking place between the second diphenylamino group and the  $\pi^*$  MOs of the TCBD or fluorenyl fragments. Higher-energy transitions (around 300 nm and shorter wavelengths) involve additional CT transitions from the second diphenylamino group and  $\pi^*$  MOs of the fluorenyl, as well as  $\pi^* \leftarrow \pi$  transitions more localized on the triphenylamino fragments.

In comparison, their precursors **4-6** are much more transparent in the visible range (Figure 2b). Again, according to the DFT calculations (see the Supporting Information), their yellowish color originates from two transitions with significant  $\pi$ - $\pi^*$  character corresponding to a CT transition from the diphenylamino end group toward the fluorenyl group. The transition at lowest energy corresponds to the HOMO-LUMO transition; its large  $\pi$ - $\pi^*$  character is supported by the very weak solvatochromism exhibited by this band for **4-6** (see



the Supporting Information). The dipole change associated with this transition is obviously rather weak.

**Table 1.** Electrochemical Data for **1-6**.<sup>[a]</sup>

Cmpd/ <u>E° [<math>\Delta E_p</math>]<sup>[b]</sup></u>	<u>2<sup>nd</sup> reduction of TCBD</u>	<u>1<sup>st</sup> reduction of TCBD</u>	<u>1<sup>st</sup> oxidation of ArNPh<sub>2</sub></u>	<u>2<sup>nd</sup> oxidation of ArNPh<sub>2</sub></u>
<b>1</b>	-0.77 [1.1]	-0.41 [0.9]	1.31 [0.8] <sup>[c]</sup>	/
<b>2'</b>	-0.76 [1.1]	-0.40 [0.9]	1.00 [0.7]	1.31 [1.0] <sup>[c]</sup>
<b>2</b>	-0.79 [1.1]	-0.42 [0.9] -0.35 [0.9]	1.30 [0.9] <sup>[c]</sup>	/
<b>3</b>	-0.79 [1.3]	-0.42 [0.9]	0.99 [0.7]	1.31 [0.9] <sup>[c]</sup>
<b>4</b>	/	/	/	0.96 [0.8]
<b>5</b>	/	/	/	0.98 [0.7]
<b>6</b>	/	/	0.84 [0.6]	0.98 [0.7]

[a] Conditions: CH<sub>2</sub>Cl<sub>2</sub> solvent, 0.1 M [<sup>n</sup>Bu<sub>4</sub>N][PF<sub>6</sub>], 20 °C, Pt electrode, sweep rate 0.100 V s<sup>-1</sup>. [b]  $\Delta E_p$  is the peak-to-peak separation; E° and  $\Delta E_p$  values in V ( $\pm$  5 mV) vs. SCE. [c] Chemically not reversible.

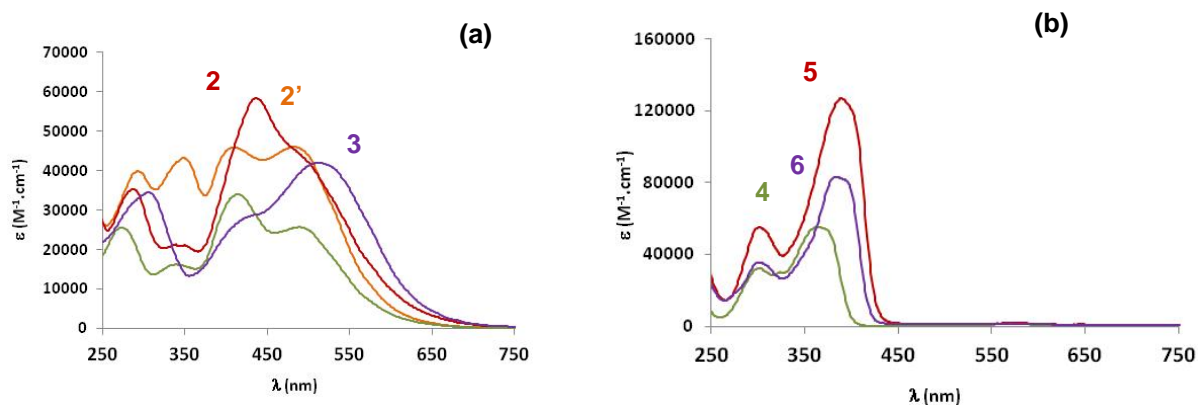


**Figure 2.** UV-Vis spectra of **1-3** (a) and **4-6** (b) in CH<sub>2</sub>Cl<sub>2</sub> at 25 °C.

**Emission studies.** In line with the scant luminescence data available for such compounds,<sup>[13a,b]</sup> the TCBD derivatives **1-3** and **2'** were found to be totally nonemissive in solution at 25 °C (Table 2). This behavior can be traced back to the fact that their lowest singlet excited state is presently a CT state mostly localized on the TCBD. Indeed, as recently demonstrated by Diederich and Armaroli,<sup>[13c]</sup> the latter often leads to rapid nonradiative deactivation by bond twisting motions via so called "twisted intermolecular charge transfer" (TICT) excited states.<sup>[22]</sup> In contrast, and unsurprisingly considering the literature on related carbon-rich organic luminophores incorporating fluorenyl fragments,<sup>[10c,20]</sup> a strong fluorescence ( $\Phi_{em} \geq 78\%$ ) was found for the precursor compounds **4-6**. Both the lifetimes, which remain in the ns range, and the observed Stokes shifts (4030, 3320, and 2930 cm<sup>-1</sup>, respectively) are consistent with reported values for this kind of compound, as is the marked positive solvatochromism found for this emission (see the Supporting Information).<sup>[10c]</sup>

**Table 2.** Absorption, CV and Emission Data for **1-6** in CH<sub>2</sub>Cl<sub>2</sub> at 25 °C.

Cmpd	Absorption	$\lambda^{S1 [a]} / \Delta G_{CT}$	Emission [c,d]	$\tau_{em} [e]$
	$\lambda$ (nm) [ $\epsilon$ ( $10^3 M^{-1} \cdot cm^{-1}$ )]	<sup>[b]</sup> (eV)	$\lambda_{em}$ (nm) [ $\Phi_{em}$ ]	(ns)
<b>1</b>	274 [24.9], 340 [15.9], 414 [33.9], 489 [25.3]	2.54 / 1.46	/	/
<b>2'</b>	293 [39.9], 349 [43.2], 410 [45.9], 483 [46.1]	2.57 / 1.30	/	/
<b>2</b>	287 [37.2], 340 [21.3], 437 [58.5], 485 [sh, 45.3]	2.56 / 1.39	/	/
<b>3</b>	306 [34.5], 441 [29.0, sh], 512 [40.1]	2.42 / 1.25	/	/
<b>4</b>	302 [32.5], 324 [30.1], 365 [55.1]	/	428 [0.78]	1.5
<b>5</b>	301 [55.1], 390 [126.8]	/	448 [0.85]	1.1
<b>6</b>	301 [35.6], 385 [83.2]	/	434 [0.84]	1.2

[a] Energy of the first allowed absorption. [b] Computed according to eq. 1 (see text). [c] Emission wavelength upon excitation of the lowest absorption peak and associated quantum yield. [d] Fluorescence quantum yield determined relative to quinine bisulfate in 0.5 M H<sub>2</sub>SO<sub>4</sub>.<sup>[21]</sup> [e] Luminescence lifetime.

**Table 3.** Absorption and Emission Data for **1-3** and **2'** in ethanol at 77 K.

Cmpd	Absorption	Emission <sup>[a,b]</sup>	$\tau_{em}$ (ns) <sup>[c]</sup>
	$\lambda$ (nm)	$\lambda_{em}$ (nm/eV) [ $\Phi_{em}$ ]	
<b>1</b>	268, 334, 406, 479	664 / 1.86 [0.12]	$\tau_1 = 6.0$ (76%), $\tau_2 = 0.9$ ns (24%)
<b>2'</b>	292, 345, 398, 469	684 / 1.81 [0.11]	$\tau_1 = 5.7$ (61%), $\tau_2 = 1.9$ (39%)
<b>2</b>	279, 337, 419, 474 (sh)	682 / 1.82 [0.08]	$\tau_1 = 5.5$ (61%), $\tau_2 = 0.8$ (39%)
<b>3</b>	301, 419 (sh), 495	696 / 1.81 [0.06]	$\tau_1 = 3.3$ (40%), $\tau_2 = 0.4$ (60%)

[a] Emission wavelength upon excitation at the lowest absorption peak, and associated quantum yield. [b] Fluorescence quantum yield determined against rhodamine 101 in EtOH at 77K ( $\Phi_F = 1$ ).<sup>[21]</sup> [c] Luminescence lifetimes (contributing percentages).

We then probed the luminescence of TCBD derivatives **1--3** and **2'** in ethanol glasses at 77 K. Under such conditions, these compounds luminesce (Figure 3a) with quantum yields in the range 6-12% (Table 3), a feature not previously observed with closely related derivatives under similar conditions.<sup>[13b]</sup> Then, monitoring their luminescence decay at 77 K revealed a multiexponential process requiring at least two time constants to be properly fitted, with lifetimes in the ns range (Table 3). This confirms that fluorescence, rather than

phosphorescence, is observed and indicates the presence of two (or more) emitting species or states in the EtOH glass at 77 K. Note however that even at 77 K, no fine structure is apparent, nor any other diagnostic change in the bandshape of the emission bands that would indicate the existence of several overlapped peaks.

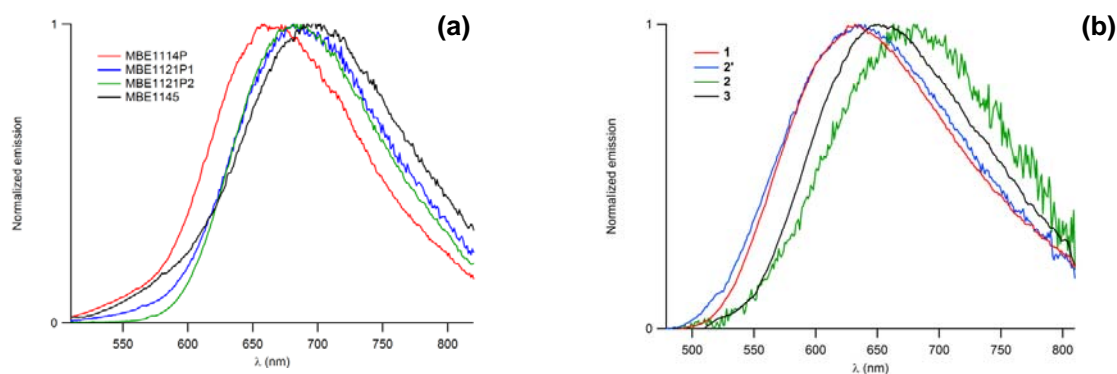


**Figure 3.** Emission spectra of **1-3** and **2'** in EtOH at 77K (a) and in SOA glass at 298 K (b).

To find out if the restored fluorescence was attributable to the lower temperature or to the increased viscosity of the medium, we next probed the luminescence of **1-3** and **2'** in sucrose octacetate (SOA) at 298 K, which gives rigid glasses at ambient temperatures.<sup>[23]</sup> Again, fluorescence was observed in a close wavelength range for each sample (Figure 3 b), but with halved (**1**, **2'**, **3**) or even lower (**2**) quantum yields (Table 4). The hypsochromic shifts observed for both the first absorptions and emissions of all compounds when proceeding from EtOH to SOA glasses (Supporting Information) can easily be rationalized by considering the positive solvatochromism usually observed for such CT transitions along with the lower dielectric constant of SOA relative to EtOH. Indeed, the former is conveniently approximated by that of ethyl acetate.<sup>[23]</sup> To the best of our knowledge, the fluorescence quantum yields found for **1-3** and **2'** in SOA glasses are among the largest ever reported so far for TCBD derivatives at ambient temperatures.<sup>[13a]</sup> The increased rigidity of the surrounding medium must be (at least in part) at the origin of this phenomenon. In line with Amarolli and

## Full Paper

Diederich's work previously mentioned,<sup>[13c]</sup> such a behavior is often diagnostic of the intermediacy of TICT states during relaxation.<sup>[22,23]</sup> Lifetime measurements further substantiate the strong similarities between the emitting state(s) for a given compound in SOA and EtOH glasses, in spite of the difference in temperature. In both cases, the existence of mainly two emitting species/states in close proportions (compare Tables 3 and 4) with different lifetimes but unresolved emission is evidenced. The observation of multiexponential fluorescence decay for a pure luminophore in SOA has precedence. This phenomenon was previously attributed to the existence of families of conformers locked within the glassy matrix.<sup>[23]</sup>

To learn more about the nature of the emitting states at room temperature the Stokes shifts and  $\lambda_{0-0}$  values were determined from the spectral data obtained in SOA glasses (Supporting Information). These "apparent" figures are evidently averaged over the various emitting states and must therefore be considered with caution. First, the Stokes shifts found for **1-3** and **2'** (5054, 5783, 4623, and 5619  $\text{cm}^{-1}$ , respectively) are 25-70% larger than those found for **4-6**. In accordance with the rare examples of fluorescence reported so far for TCBD derivatives in solution,<sup>[13a]</sup> these values reveal that a significant structural reorganization takes place during the relaxation process. Then, the  $\lambda_{0-0}$  energies of 2.14-2.27 eV found indicate that the (singlet) emitting state(s) should be around 0.9 eV higher in energy than the CT state at lowest energy for which the energies have been derived in  $\text{CH}_2\text{Cl}_2$  (Table 2). Correcting these energies for the change in polarity between  $\text{CH}_2\text{Cl}_2$  and SOA only marginally reduces this energy gap ( $\Delta G_{\text{CT}}=1.47, 1.41, 1.32,$  and  $1.40$  eV for **1-3** and **2'** in SOA).<sup>[13b]</sup> Furthermore, even the various  $\lambda_{\text{em}}$  energies corresponding to the emission maxima in the SOA glasses (Table 4) are around 0.5 eV higher than these values. These observations strongly suggest that most of the emitting states (if not all) are significantly higher in energy than the fully relaxed CT state, which correspond to the TICT state.<sup>[22b]</sup> The present MO calculations (see later) indicate however that these luminescent state(s), likewise to the TICT state, result from an initial  $(\pi^*)_{\text{TCNE}} \leftarrow (\pi)_{\text{FluNPh}_2}$  photoinduced charge transfer. Therefore they likely correspond to the (vertical) untwisted CT state. Notably, based on the  $\Delta G_{\text{CT}}$  determined for the various

TCBD derivatives in SOA, we also want to stress that the corresponding TICT states should emit in the 850-50 nm region, thus outside the detection range of our fluorimeter.

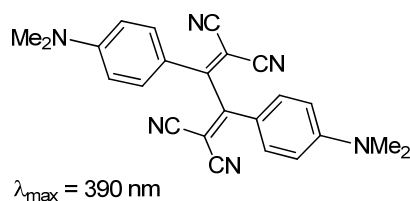
**Table 4.** Absorption and Emission Data for **1-3** and **2'** in sucrose octaacetate (SOA) glass at 298 K.

Cmpd	Absorption	Emission <sup>[a,b]</sup>	$\tau_{em}$ (ns) <sup>[c]</sup>
	$\lambda$ (nm)	$\lambda_{em}$ (nm/eV) [ $\Phi_{em}$ ]	
<b>1</b>	325, 405, 479	632 / 1.96 [0.06]	$\tau_1 = 5.3$ (66%), $\tau_2 = 1.6$ ns (34%)
<b>2'</b>	352, 396, 468	635 / 1.95 [0.05]	$\tau_1 = 5.3$ (57%), $\tau_2 = 1.6$ (43%)
<b>2</b>	420, 486 (sh)	676 / 1.83 [0.02]	$\tau_1 = 5.2$ (57%), $\tau_2 = 1.0$ (43%)
<b>3</b>	412, 501	652 / 1.90 [0.06]	$\tau_1 = 5.0$ (64%), $\tau_2 = 1.7$ (36%)

[a] Emission wavelength upon excitation at the lowest absorption peak, and associated quantum yield. [b] Fluorescence quantum yield determined against rhodamine 101 in EtOH ( $\Phi_F = 1$ ).<sup>[21]</sup> [c] Luminescence lifetimes (contributing percentages).

Based on present work and on calculations of Diederich and Amarolli,<sup>[13c]</sup> we tentatively propose that the radiative relaxation proceeds from the first singlet excited state of **1-3** and **2'**, assuming that it corresponds to the vertical CT state. Relaxation would operate from this state via a twisting motion of one of the aromatic units connected to the TCBD unit. Consistent with this hypothesis, increasing the viscosity of the matrix would restore the fluorescence by slowing down these rotational motions. Relaxation would proceed through the TICT state leading eventually to the ground state (GS) by back electron transfer, but

emission from the TICT state cannot be probed under our experimental conditions. Finally, the photogeneration of two (or more) distinct emissive states most probably corresponds to different conformers, rigidly trapped in the solvent glass.



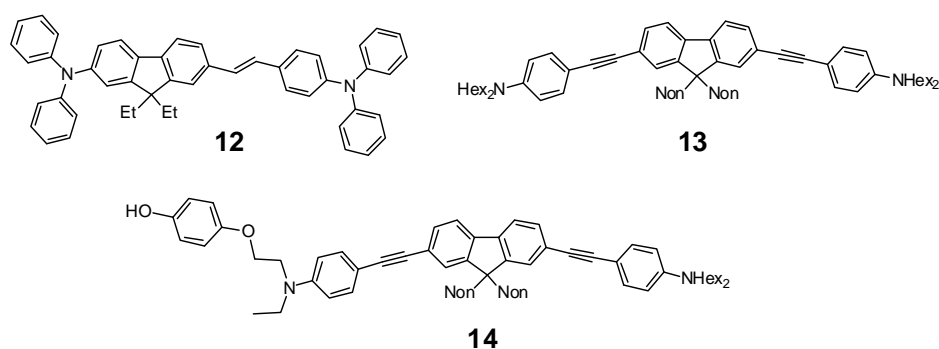
**11**

**Scheme 3.** Quadrupolar TCBD derivative related to **2** and **3**.

A closer look at our data reveals that the most fluorescent species are **1** and **2'** in ethanol glasses at 77 K. When compared to **11** (Scheme 3), which is not fluorescent in solvent glasses at 77 K,<sup>[13b]</sup> it seems that by replacing of one 4-dimethylaminophenyl groups in **11** with a less electron-rich aromatic group such as 2-fluorenyl or 2-(7-diphenylamino)fluorenyl and by replacing the remaining dimethylamino unit with the less electron-releasing diphenylamino donor is sufficient enough to restore some fluorescence in rigid media at room temperature. Considering that the triaryl-amino donor groups in **1** and **2'** are more bulky and therefore certainly more prone to be influenced by the viscosity of the surrounding medium during relaxation, steric factors might be at the origin of that change. Alternatively, based on CV data ( $E^{\circ}_{\text{Ox}} - E^{\circ}_{\text{Red}} = 1.92 \text{ eV}$  in  $\text{CH}_2\text{Cl}_2$ ),<sup>[13a]</sup> both **1** and **2'** also give lower  $\Delta G_{\text{CT}}$  values than **11**, meaning that a smaller driving force for charge recombination is operative for these compounds. At this stage, further studies are needed to unambiguously determine if the restored fluorescence of **1-3** and **2'** in solvent glasses can be dominantly attributed to steric or electronic factors.



**Two-photon emission studies.** The 2PA cross-sections (Table 5) at 25 °C were next determined for **4-6** using two-photon excited fluorescence (TPEF). The highest values are found for the quadrupolar derivative **5**, followed by that of the multipolar derivative **6** possessing two distinct diphenylamino donor groups, while the purely dipolar derivative **4** is clearly less active. The 2PA cross-section for **6** is significantly larger than that obtained for its ethynyl analogue **12** by TPEF, for which a value of 282 GM at 730 nm had been reported in toluene solutions.<sup>[20]</sup> Surprisingly,<sup>[10c,7b,9]</sup> this suggests that the ethynyl bridge is better than the 1,2-ethynyl unit in promoting 2PA in such compounds.



**Scheme 4.** Selected two-photon absorbers related to **5** and **6**.

For **4**, the match between the absorption maxima in the 2PA and one-photon absorption (1PA) spectra divided by two is excellent (Supporting Information), indicating that 1PA takes place in the lowest one-photon-allowed excited state. In contrast, the 2PA band maximum for **5** is observed at a somewhat higher energy than that of the lowest-lying allowed one-photon absorption divided by two. This can be related to the different selection rules operating for one- and two-photon absorptions in this centrosymmetric quadrupolar chromophore, resulting in a larger 2PA cross-section for the one-photon forbidden and two-photon allowed state.<sup>[10c]</sup> In line with measurements reported for **12**,<sup>[20]</sup> it seems that a somewhat similar situation prevails in the case of the noncentrosymmetric multipolar derivative **6** (Supporting Information), although both excited states should be now one-photon allowed. Notably, **5** performs slightly better than both its dihexylamino/nonyl analogue **13** (Scheme 4)<sup>[10c]</sup> and its dissymmetric analogue **14**, while possessing a slight redshifted

absorption maximum (720 vs.  $703 \pm 2$  nm for **13** and **14**; see the Supporting Information).<sup>[10f]</sup> In terms of applications, **4** and **6** are potentially interesting as photoinitiators for nanofabrication, while **5** may be of interest for bioimaging purposes,<sup>[7b]</sup> or even optical limiting/rectification in the near-IR range.<sup>[24]</sup>

**Z-scan studies.** We then examined **1-3** and **2'** by Z-scan to determine their cubic nonlinear optical properties. The molecular third-order NLO coefficients of these compounds in the near-IR domain are dominated by their real parts ( $\gamma_{Re}$ ) which are overall negative (Supporting Information). Due to dispersion, very large negative peaks are observed near 1250 nm, except for **2'** for which a positive peak is present instead (Table 6). At longer wavelengths, these values converge to negative values of much lower magnitude. Unfortunately, the fairly large experimental uncertainty forbids their accurate evaluation, but their magnitude is in the range previously determined at 1500 nm ( $6 \times 10^{-48} \text{ m}^5 \cdot \text{V}^{-2}$  or  $43 \times 10^{-35}$  esu) by four-wave mixing (DFWM) for related polycyano derivatives such as **15** (Scheme 5), at least for **2**, **3** and **2'**.<sup>[3,6]</sup> When taking into consideration either the number of active electrons<sup>[25]</sup> or the molecular mass of the compounds,<sup>[3a]</sup> the asymmetric derivative **3** appears to be the most active among **1-3** in the spectral range investigated. Notably, comparison with **1** reveals that the inclusion of a second donor site is essential to promote a large cubic NLO activity in the near-IR range.

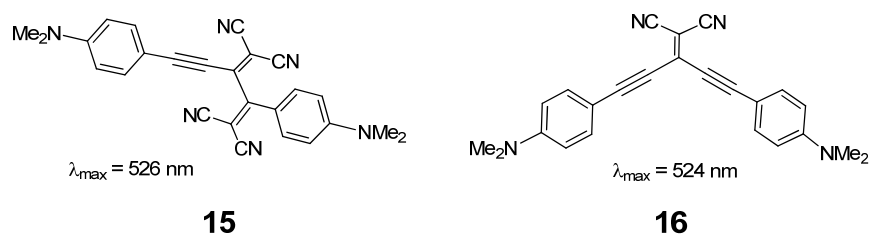
We next sought to determine their 2PA cross-sections from the open-aperture measurements (Table 5). For **1** and **3**, Z-scan reveals only one maximum in the near-IR range which matches with half of the energy of the dominant one-photon peak detected in the visible range, whereas for **2** and **2'** (Figure 4 and Supporting Information), essentially two maxima are revealed which likewise correspond to half of the energy of the strongest one photon-allowed transitions at lowest energy. For **2** and **2'**, several additional weak 2PA peaks (50-100 GM) can be detected at lower energies. These peaks most likely correspond to excited states at the red edge of the main absorption band with low oscillator strengths. According to previous results and DFT calculations (see later), they probably correspond to excited CT states associated with HOMO-LUMO transitions in more energetic (twisted)

conformations. These 2PA values are all larger than that previously reported for the related derivative **16** (88 GM) at 900 nm.<sup>[7a]</sup>

**Table 5.** 2PA maximal values of **1-6** in dichloromethane at 25 °C determined by TPEF or Z-scan.

Cmpd	$\lambda_{\text{OPA}}$ <sup>[a]</sup>	$\lambda_{2\text{PA}}$ <sup>[b]</sup>	$\sigma_2$ <sup>[c]</sup>	$\sigma_{2,\text{max}}/MW$ <sup>[d]</sup>	$\Phi \cdot \sigma_2$ <sup>[e]</sup>
/method	(nm)	(nm)	(GM)	(GM/g)	(GM)
<b>1</b> /Z-scan	489	925 <sup>[f]</sup>	115 <sup>[f]</sup>	0.17 <sup>[f]</sup>	/
<b>2</b> /Z-scan	415/488	800/950	170/210	0.16/0.20	/
<b>2'</b> /Z-scan	410/483	850/950	330/310	0.35/0.33	/
<b>3</b> /Z-scan	512	1050	390	0.46	/
<b>4</b> /TPEF	365	750	140	0.27	109
<b>5</b> /TPEF	391	720	980	1.21	833
<b>6</b> /TPEF	385	700	540	0.76	454

[a] One-photon absorption corresponding to the detected 2PA maximum. [b] Maximal value of the two-photon absorption ( $\pm \leq 10\%$ ). [c] 2PA cross-sections measured by TPEF in the femtosecond regime. TPEF cross-sections were measured relative to fluorescein in 0.01 M aqueous NaOH over the range 715-980 nm,<sup>[17]</sup> with the appropriate solvent-related refractive index corrections.<sup>[18]</sup> Data points between 700 and 715 nm were corrected according to ref. [10e] [d] Figure-of-merit relevant for applications in optical limiting or nanofabrication.<sup>[9b]</sup> [e] Two-photon brightness relevant figure-of-merit for imaging applications.<sup>[19]</sup> In these expressions,  $MW$  represents the molecular weight and  $\Phi$  the luminescence quantum yield. [f] Determined in THF.



**Scheme 5.** Selected poly-cyano derivatives related to **1-3** for which cubic NLO have been determined.

Thus, among **1-3**, the most active two-photon absorber is the multipolar compound **3**, followed by the nonsymmetric compound **2'**. Both perform significantly better than the symmetric compound **2** or the shorter nonsymmetric compound **1**. This might be traced back to the preservation of extended  $\pi$ -conjugated segments between donor (diphenylamino) and acceptor (TCBD) sites in **2'** and **3**. Indeed, replacement of the alkyne spacer by TCBD units, while multiplying the possible intramolecular CT pathways, also disrupts  $\pi$ -conjugation between the two sides of the molecule. When compared with 2PA data obtained for **4-6** by TPEF, the 2PA cross-section maximal values for **1-3** and **2'** are lower than those of their precursors, revealing that the inclusion of the TCBD unit in these structures is actually detrimental to their two-photon cross-sections.<sup>[27]</sup> Moreover, a clear loss of transparency in the visible range occurs upon progressing from **4-6** to **1-3** and **2'**, which originates from the numerous low-energy CT excited states generated by insertion of TCNE in the alkyne spacer.

In terms of applications,<sup>[28]</sup> their overall good third-order activity and sizeable 2PA activity make them suited for applications such as optical-limiting in the near-IR range,<sup>[29]</sup> beam reshaping in the far-IR range and evidently for applications not related to their transparency, such as two-photon sensitization for nanolithography or photodynamic therapy.<sup>[7b]</sup> Furthermore, compared to other purely organic structures envisioned for such applications, their remarkable redox activity constitutes an additional and important key feature which might open new opportunities for using them in electro-optic devices in the future.<sup>[30]</sup>

**Table 6.** Selected third-order NLO data for **1-3** and **2'** determined in dichloromethane at 25 °C by Z-scan.

<u>Cmpd</u>	<u><math>\lambda</math> at <math>\gamma_{\max}</math> [a]</u>	<u><math>N</math> [b]</u>	<u><math>(\gamma_{re})_{\max}</math> [c]</u>	<u><math> \gamma_{\max} /1400</math> [d]</u>	<u><math>\gamma_{\max}/MW</math> [e]</u>
	(nm)		( $10^{-36}$ esu)	( $10^{-36}$ esu)	( $10^{-36}$ esu/g)
<b>1</b> [f]	1100	23.2	$-394 \pm 35$	$385 \pm 55$	0.6
<b>2</b>	1250	31.8	$-15100 \pm 410$	$15100 \pm 450$	14.1
<b>2'</b>	1250	31.0	$13900 \pm 290$	$13900 \pm 310$	14.8
<b>3</b>	1250	24.7	$-13500 \pm 200$	$13500 \pm 200$	16.1

[a] Wavelength of the maximal value of  $\gamma_{Re}$  in the near-IR range. [b] Number of active  $\pi$ -electrons. [25-26] [c] Minimal value of the real part of  $\gamma$  in the 800-1600 nm range, as determined from closed-aperture Z-scan measurements. [d] Maximum  $\gamma$  value derived. [e] *Specific*  $\gamma$  value,  $MW$  represents the molecular weight. [f] Determined in THF.

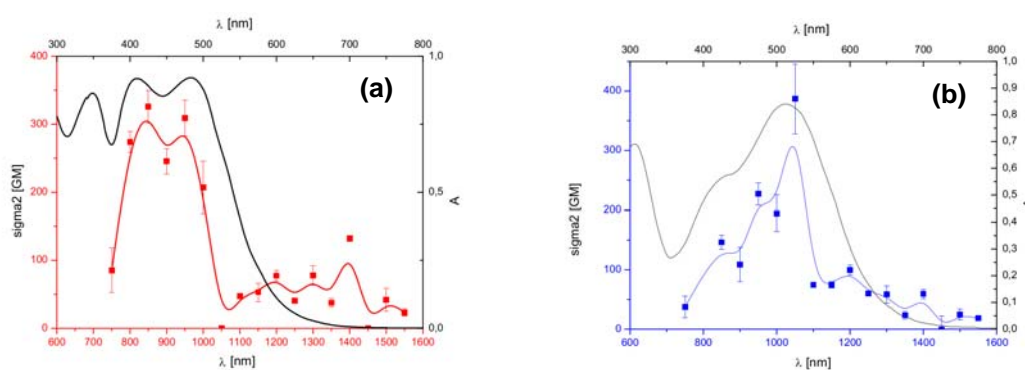


**Figure 4.** Overlay of one and two-photon absorption spectra for **2'** (a) and **3** (b) in  $\text{CH}_2\text{Cl}_2$  at 25 °C. The two-photon cross-sections are derived from open-aperture Z-scan measurements and the one-photon spectra are plotted against twice the wavelength ( $2\lambda$ ).

**DFT calculations.** The compounds were modeled using DFT on simplified models without the butyl chains on fluorenyl (**C1--C6**). To assist attribution of the IR and UV/Vis absorption spectra recorded for **1--6**, modelling of the IR absorptions was performed for **C1-C6**, as well as time-dependent (TD)DFT calculations. Once scaled using the proper factor to correct for anisotropy (0.951),<sup>[31]</sup> the computed vibrational spectra reproduced satisfyingly (see the Supporting Information) the most characteristic vibrational modes of **1-6** and helped us in the assignment of the characteristic stretching modes of these molecules, while TD-DFT calculations reproduced the experimentally observed spectra within 0.3 eV (Table 7).

As expected, the match is less satisfactory for electronic transitions involving long-range charge transfer when employing such a functional that does not incorporate long-range corrections.<sup>[32]</sup> The calculations are nevertheless sufficient to provide a qualitative understanding of the origin of the excited states underlying the absorptions of **1-3**. Furthermore, we verified in selected cases that the observed discrepancies do not originate from different conformers than the ones computed, a distribution of these being certainly present in solution. Indeed, a nearly similar spectral shape was obtained in each case for various low-energy rotamers of the TCBD single bonds modeled by TD-DFT (see the Supporting Information).

For **C1-C3**, the HOMO is mostly located on the triphenylamino fragment and the HOMO-1 either on the fluorenyl fragment (**C1**) or on the triphenylamino fragments (**C2-C3**), whereas the LUMO and LUMO-1 are strongly located on the TCBD fragment(s). In line with our CV data (Table 1), the calculations thus confirm that an electron mostly located on the triphenylamino group will be ionized first upon oxidation, whereas reduction will result in the injection of an electron into the  $\pi^*$  of the TCBD units. Unsurprisingly, the allowed (singlet-singlet) transitions are LUMO $\leftarrow$ HOMO and have a strong CT character in **1--3**, as briefly mentioned above (Table 6). The next lowest-energy transitions in these derivatives apparently involve transitions more localized on the fluorenyl or triphenylamino fragments.

**Table 7.** Experimental vs. Computed <sup>[a]</sup> (PBE0 / 6-31G) Values (nm). Energy and Composition of the First Singlet Excited States (Wavelength, Oscillator Strength  $f$ , Transition Percentage)

Cmpd	Experimental $\lambda_{\max}$ [ $\epsilon$ ] <sup>[b]</sup>	Calculated <sup>[c]</sup> $\lambda_{\max}$ [ $f$ <sup>[d]</sup> ]	Composition	Major Assignment <sup>[e]</sup>
<b>1</b>		544 [0.16]	154 → 155 (96%)	$(\pi^*)_{\text{TCNE}} \leftarrow (\pi)_{\text{PhNPh}_2}$
	489 [25.3]	432 [0.26]	153 → 155 (94%)	$(\pi^*)_{\text{TCNE}} \leftarrow (\pi)_{\text{Flu}}$
	414 [33.9]	418 [0.54]	154 → 156 (92%)	$(\pi^*)_{\text{Flu/TCNE}} \leftarrow (\pi)_{\text{PhNPh}_2}$
	340 [15.9]	358 [0.42]	153 → 156 (92%)	$(\pi^*)_{\text{Flu/TCNE}} \leftarrow (\pi)_{\text{Flu}}$
	274 [24.9]	280 [0.14]	154 → 160 (62%)	$(\pi^*)_{\text{Flu}} \leftarrow (\pi)_{\text{PhNPh}_2}$
<b>2</b>	/	599 [0.11]	256 → 257 (87%)	$(\pi^*)_{\text{TCNE/Flu}} \leftarrow (\pi)_{\text{PhNPh}_2}$
	485 [45.3]	499 [0.12]	256 → 258 (88%)	$(\pi^*)_{\text{TCNE}} \leftarrow (\pi)_{\text{PhNPh}_2}$
	437 [58.5],	437 [1.02]	254 → 257 (82%)	$(\pi^*)_{\text{TCNE/Flu}} \leftarrow (\pi)_{\text{Flu}}$
	/	422 [0.56]	255 → 259 (86%)	$(\pi^*)_{\text{TCNE/Flu}} \leftarrow (\pi)_{\text{PhNPh}_2}$
	340 [21.3]	383 [0.12]	255 → 260 (80%)	$(\pi^*)_{\text{TCNE}} \leftarrow (\pi)_{\text{PhNPh}_2}$
	/	359 [0.11]	253 → 257 (71%)	$(\pi^*)_{\text{TCNE/Flu}} \leftarrow (\pi)_{\text{PhNPh}_2}$
	287 [37.2]	288 [0.11]	252 → 259 (51%)	$(\pi^*)_{\text{TCNE/Flu}} \leftarrow (\pi)_{\text{PhNPh}_2}$
	/	277 [0.10]	244 → 258 (63%)	$(\pi^*)_{\text{TCNE}} \leftarrow (\pi)_{\text{NPh}_2}$
<b>2'</b>		647 [0.32]	224 → 225 (99%)	$(\pi^*)_{\text{TCNE}} \leftarrow (\pi)_{\text{NPh}_3}$
		549 [0.17]	223 → 225 (96%)	$(\pi^*)_{\text{TCNE}} \leftarrow (\pi)_{\text{NPh}_3}$

Full Paper

	483 [46.1]	488 [0.42]	224 → 226 (96%)	$(\pi^*)_{\text{TCNE/Flu}} \leftarrow (\pi)_{\text{NPh}_3}$
	/	456 [0.38]	222 → 225 (94%)	$(\pi^*)_{\text{TCNE}} \leftarrow (\pi)_{\text{Flu/NPh}_3}$
	410 [45.9]	419 [0.55]	223 → 226 (93%)	$(\pi^*)_{\text{TCNE/Flu}} \leftarrow (\pi)_{\text{NPh}_3}$
		377 [0.83]	222 → 226 (69%)	$(\pi^*)_{\text{TCNE/Flu}} \leftarrow (\pi)_{\text{Flu/NPh}_3}$
	349 [43.2]	366 [0.36]	224 → 227 (66%)	$(\pi^*)_{\text{Flu}} \leftarrow (\pi)_{\text{NPh}_3}$
	293 [39.9]	299 [0.16]	224 → 233 (80%)	$(\pi^*)_{\text{NPh}_2} \leftarrow (\pi)_{\text{NPh}_3}$
		291 [0.17]	222 → 227 (52%)	$(\pi^*)_{\text{Flu}} \leftarrow (\pi)_{\text{Flu/NPh}_3}$
<b>3</b>	512 [40.1]	606 [0.32]	198 → 199 (99%)	$(\pi^*)_{\text{TCNE}} \leftarrow (\pi)_{\text{NPh}_3}$
		533 [0.16]	197 → 199 (96%)	$(\pi^*)_{\text{TCNE}} \leftarrow (\pi)_{\text{NPh}_3}$
	441 [29.0, sh]	473 [0.38]	198 → 200 (96%)	$(\pi^*)_{\text{TCNE/Flu}} \leftarrow (\pi)_{\text{NPh}_3}$
	/	418 [0.54]	197 → 200 (94%)	$(\pi^*)_{\text{TCNE}} \leftarrow (\pi)_{\text{FluNPh}_2}$
		387 [0.17]	196 → 199 (94%)	$(\pi^*)_{\text{TCNE/Flu}} \leftarrow (\pi)_{\text{FluNPh}_2}$
		333 [0.15]	196 → 200 (42%)	$(\pi^*)_{\text{TCNE/Flu}} \leftarrow (\pi)_{\text{FluNPh}_2}$
			193 → 199 (21%)	$(\pi^*)_{\text{TCNE}} \leftarrow (\pi)_{\text{PhNPh}_2}$
	306 [34.5]	327 [0.15]	195 → 199 (36%)	$(\pi^*)_{\text{TCNE}} \leftarrow (\pi)_{\text{PhNPh}_2}$
		296 [0.15]	198 → 205 (67%)	$(\pi^*)_{\text{NPh}_2} \leftarrow (\pi)_{\text{FluNPh}_2}$

[a] The calculated excited states are  $^1\text{A}$ . [b] Experimental absorption (nm) and extinction coefficients ( $\epsilon$ ) in  $10^3 \text{ M}^{-1} \cdot \text{cm}^{-1}$ . [c] in nm. [d] Computed transition moment under vacuum. [e] See ESI for the plot of the corresponding MOs.



Regarding their alkynyl precursors (**C4-C6**), the HOMO is also strongly localized on the triphenylamino fragment, while the LUMO is a  $\pi^*$  MO on the fluorenyl and alkynyl ligand(s). Thus, the first allowed transition at lowest energy is a  $\pi^* \leftarrow \pi$  transition with some CT character (Supporting Information, Table S4). Again, the next lowest-energy transitions in these derivatives apparently involve transitions more localized on the fluorenyl or triphenylamino fragments.

Note that the calculated transition moments for the (long-range) CT transitions at lowest energy are somewhat overestimated, as is sometimes the case for long-range charge transfer.<sup>[32]</sup> As a result, the red side of the simulated spectra is slightly more intense than experimentally observed, especially for **2'** and **3**. The existence of poorly allowed CT transitions on the red side of the main absorption peak observed in the 600-700 nm spectral range is also attested by the presence of sizeable 2PA in the 1200-1400 nm range. In line with literature,<sup>[1,13c]</sup> calculations indicate that these will correspond to excitations from the most electropositive triphenylamino donor toward the TCBD acceptor(s), but for molecules having more energetic conformations than for the GS.

## Conclusion

We have reported the synthesis and characterization of four new TCBD derivatives (**1-3** and **2'**) featuring fluorenyl and triaryl amino groups. While exhibiting the characteristic electroactivity expected for TCBDs and triaryl amino-containing derivatives, we show here that none of these multipolar derivatives are fluorescent in solution at ambient temperatures, in contrast to their alkyne precursors (**4-6**). However, **1-3** and **2'** were shown to be fluorescent in solvent glasses. This unprecedented finding is important, since it potentially opens an access to fluorescent materials by embedding these derivatives in rigid matrices. The 2PA

properties of these conjugated derivatives have been investigated by TPEF or Z-scan and it was shown that **1-3** and **2'** are two-photon absorbers into their lowest excited states with **3** being the most active among them. 2PA takes place deep in the near-IR range, but their cross-sections are lower than for their corresponding precursors (**4-6**), in line with the diminished fluorenyl character of the corresponding excited states. Thus, cycloaddition of TCNE at **4-6** constitutes a simple means to shift both the linear and nonlinear absorption maxima to lower energies. The refractive third-order NLO properties of **1-3** and **2'** have also been investigated. Similar to the few TCBD derivatives previously investigated, the fair cubic NLO activities in the near-IR range make them worthy of consideration for various applications in the near/far-IR range, such as optical limiting, pulse reshaping, or two-photon photosensitization. Furthermore, the remarkable redox activity of these all-organic structures combined with their specific cubic NLO activity in the near-IR range might open new opportunities for their applied use in the future.

In terms of molecular design, the present study suggests that third-order NLO properties might be even more favored in related derivatives presenting an extended and electron-rich  $\pi$ -manifold on the external fluorenyl side, while luminescence seem to be favored in derivatives lacking a second amino group on this part, such as in **1**, or having it further removed from the TCBD core, such as in **2'**. Also, keeping an overall centrosymmetry, such as in **2**, does apparently not constitute a decisive structural feature for improving further these properties.

## Experimental Section

**General.** All reactions and work-up procedures of air-sensitive compounds were carried out under dry, high-purity argon or nitrogen, using standard Schlenk techniques.<sup>[33]</sup> All glassware was oven-dried overnight at 120 °C prior to use. Solvents/reagents were dried and distilled as follows: Et<sub>2</sub>O, hexane and reagent grade THF (sodium-benzophenone), CH<sub>2</sub>Cl<sub>2</sub> (CaH<sub>2</sub>), diisopropylamine and triethylamine (KOH), and DMF (activated 3 Å molecular

sieves). Flash column chromatography was performed using silica (Acros 60 Å, 40-60 mesh). Hexane used for column chromatography refers to petroleum spirit (boiling point range 60-80 °C). *p*-(HC≡CC<sub>6</sub>H<sub>4</sub>)NPh<sub>2</sub>, (**7**)<sup>[17, 34]</sup> and 2,7-diodo-9,9-dibutylfluorene (**9**)<sup>[12, 35]</sup> were obtained as described in the literature. Other chemicals were purchased from a commercial source (Sigma-Aldrich) and used as received.

**Instrumentation.** Melting points were taken in air using a melting point apparatus. Infrared spectra were obtained as KBr disks in the 400-4000 cm<sup>-1</sup> range. Raman spectra were obtained from the solid samples by diffuse scattering in the 100-3300 cm<sup>-1</sup> range (Stokes emission) with a laser excitation source at 1064 nm (30 mW), using a quartz separator with a FRA 106 detector. NMR spectra were acquired at 298 K on 400 and/or 500 MHz FT NMR spectrometers. Cyclic voltammograms were recorded in dry CH<sub>2</sub>Cl<sub>2</sub> solutions (containing 0.1 M [N<sup>n</sup>Bu<sub>4</sub>][PF<sub>6</sub>], purged with nitrogen and maintained under an inert atmosphere) using a Pt disk as working electrode, a Pt wire as counter electrode and a SCE reference electrode; the FeCp<sub>2</sub><sup>0/+1</sup> couple (E<sub>1/2</sub>: 0.46 V,<sup>[36]</sup> ΔE<sub>p</sub> = 0.09 V; I<sub>pa</sub>/I<sub>pc</sub> = 1) was used as an internal calibrant. UV-visible-NIR spectra were recorded using a 1 cm quartz cell on a Cary 5 spectrometer, and are reported as λ<sub>max</sub> (nm) [log ε (M<sup>-1</sup> cm<sup>-1</sup>)]. Elemental analysis and unit- and high-resolution mass spectra (EI and ESI) were obtained at the Centre Regional de Mesures Physiques de l'Ouest (CRMPO) or at Wroclaw University of Technology (WUT).

**Synthesis of compound 1:** A solution of the fluorene derivative **4** (61 mg, 0.11 mmol) and TCNE (14 mg, 0.11 mmol) in CH<sub>2</sub>Cl<sub>2</sub> (1.1 mL) was stirred at 20 °C for 15 h. The reaction mixture was concentrated under reduced pressure to give the title compound (75 mg, 100%) as a dark red solid. **MP**: 108-111 °C. **R<sub>f</sub>**: 0.24 [Petroleum ether/Et<sub>2</sub>O (9:1)]. **<sup>1</sup>H NMR** (400 MHz, CDCl<sub>3</sub>) δ = 7.83 (1H, d, *J* = 1.5 Hz, H<sub>Flu</sub>), 7.72 (1H, d, *J* = 8.1 Hz, H<sub>Flu</sub>), 7.71-7.67 (1H, m, H<sub>Flu</sub>), 7.61 (2H, d, *J* = 9.3 Hz, H<sub>Ar</sub>), 7.46 (1H, dd, *J* = 1.9 and 8.1 Hz, H<sub>Flu</sub>), 7.39-7.28 (7H, m, H<sub>Ar</sub> and 3H<sub>Flu</sub>), 7.21-7.11 (6H, m, 2H<sub>Ar</sub>), 6.86 (2H, d, *J* = 9.3 Hz, H<sub>Ar</sub>), 2.03-1.85 (4H, m,

## Full Paper

$H_{Bu}$ ), 1.05-0.92 (4H, m,  $H_{Bu}$ ), 0.57 (6H, t,  $J = 7.3$  Hz,  $H_{Bu}$ ), 0.54-0.44 (4H, m,  $H_{Bu}$ ).  $^{13}C\{^1H\}$  NMR (100 MHz,  $CDCl_3$ )  $\delta = 168.9, 164.7, 153.8, 152.6, 152.3, 148.2, 144.7, 139.0, 132.1, 130.3, 130.2, 129.9, 129.4, 127.6, 127.1, 126.8, 124.5, 123.4, 122.0, 121.4, 121.0, 118.2, 113.8, 112.8, 112.8, 111.9, 85.1, 78.6, 55.8, 39.9, 26.1, 23.0, 13.9$ . IR (KBr,  $cm^{-1}$ ):  $\nu = 3061, 2928$  (m,  $C_{Ar-H}$ ), 2219 (m,  $C\equiv N$ ), 1607 (m,  $C=C$ ), 1586 (s,  $C=C_{Ar}$ ). Raman (neat,  $cm^{-1}$ ):  $\nu = 3066$  (vw,  $C_{Ar-H}$ ), 2221 (s,  $C\equiv N$ ), 1609 (s,  $C=C$ ), 1520 (vs,  $C=C_{Ar}$ ). HRMS: calculated for  $C_{47}H_{40}N_5 [M+H]^+$  674.32837, found 674.3278, calculated for  $C_{47}H_{39}N_5 M^+$  673.32055, found 673.3197. UV-vis ( $CH_2Cl_2$ ):  $\lambda_{max}$  (log  $\epsilon$ ) = 274 (4.40), 340 (4.20), 414 (4.53), 489 (4.40).

**Synthesis of compound 2:** A solution of the fluorene derivative **5** (67 mg, 0.083 mmol) and TCNE (21 mg, 0.165 mmol) in  $CH_2Cl_2$  (0.8 mL) was stirred at 20 °C for 16 h. The reaction mixture was purified by column chromatography [Petroleum ether/EtOAc (9:1) to (7:3)] to give TCBD **2** (84 mg, 95%) as a dark red solid. MP: decomposition observed above 155 °C.  $R_f$ : 0.48 [Petroleum ether/EtOAc (4:1)].  $^1H$  NMR (400 MHz,  $CDCl_3$ ):  $\delta = 7.93$  (2H, d,  $J = 1.7$  Hz,  $H_{Flu}$ ), 7.89 (2H, d,  $J = 8.1$  Hz,  $H_{Flu}$ ), 7.70 (4H, d,  $J = 9.3$  Hz,  $H_{Ar}$ ), 7.57 (2H, dd,  $J = 1.7$  and 8.1 Hz,  $H_{Flu}$ ), 7.45-7.37 (8H, m,  $H_{Ar}$ ), 7.32-7.20 (12H, m,  $H_{Ar}$ ), 6.96 (4H, d,  $J = 9.3$  Hz,  $H_{Ar}$ ), 2.15-2.00 (4H, m,  $H_{Bu}$ ), 1.13-1.00 (4H, m,  $H_{Bu}$ ), 0.64 (6H, t,  $J = 7.3$  Hz,  $H_{Bu}$ ), 0.61-0.50 (4H, m,  $H_{Bu}$ ).  $^{13}C\{^1H\}$  NMR (100 MHz,  $CDCl_3$ ):  $\delta = 168.3, 163.6, 153.8, 153.4, 144.8, 144.3, 132.2, 131.9, 130.0, 129.2, 126.9, 126.8, 124.6, 122.3, 121.3, 117.9, 113.6, 112.8, 112.2, 111.4, 87.0, 78.0, 56.4, 39.3, 25.9, 22.7, 13.7$ . IR (KBr,  $cm^{-1}$ ):  $\nu = 3036$  (m,  $C_{Ar-H}$ ), 2928 (m,  $C_{Ar-H}$ ), 2220 (m,  $C\equiv N$ ), 1608 (s,  $C=C$ ), 1586 (s,  $C=C_{Ar}$ ). Raman (neat,  $cm^{-1}$ ):  $\nu = 3067$  (vw,  $C_{Ar-H}$ ), 2222 (s,  $C\equiv N$ ), 1610 (s,  $C=C$ ), 1522 (vs,  $C=C_{Ar}$ ). HRMS: calculated for  $C_{73}H_{53}N_{10} [M+H]^+$  1069.44492, found 1069.4440, calculated for  $C_{73}H_{52}N_{10} M^+$  1068.43764, found 1068.4377. UV-vis ( $CH_2Cl_2$ ):  $\lambda_{max}$  (log  $\epsilon$ ) = 287 (5.57), 340 (4.32), 437 (4.76), 485 (4.65).

**Synthesis of compound 2':** A solution of the fluorene derivative **5** (68 mg, 0.084 mmol) and TCNE (11 mg, 0.084 mmol) in  $CH_2Cl_2$  (0.8 mL) was stirred at 20 °C for 16 h. The reaction mixture was purified by column chromatography [Petroleum ether/EtOAc (1:0) to (7:3)] to give the title compound (48 mg, 61%) and compound **2** (17 mg, 19%) as dark red

## Full Paper

solids. **MP**: 135-138 °C. **R<sub>f</sub>**: 0.92 [Petroleum ether/EtOAc (4:1)]. **<sup>1</sup>H NMR** (400 MHz, CDCl<sub>3</sub>): δ = 7.83 (1H, d, *J* = 1.6 Hz, *H*<sub>Flu</sub>), 7.70-7.71 (1H, d, *J* = 8.1 Hz, *H*<sub>Flu</sub>), 7.64 (1H, dd, *J* = 0.8 and 7.7 Hz, *H*<sub>Flu</sub>), 7.61 (2H, d, *J* = 9.3 Hz, *H*<sub>Ar</sub>), 7.48-7.46 (1H, m, *H*<sub>Flu</sub>), 7.44 (2H, br s, *H*<sub>Flu</sub>), 7.36-7.28 (6H, m, *H*<sub>Ar</sub> and *H*<sub>Flu</sub>), 7.24-7.11 (10H, m, 3*H*<sub>Ar</sub>), 7.07-7.03 (4H, m, *H*<sub>Ar</sub>), 7.00 (2H, tt, *J* = 1.1 and 7.3 Hz, *H*<sub>Ar</sub>), 6.94 (2H, d, *J* = 8.8 Hz, *H*<sub>Ar</sub>), 6.86 (2H, d, *J* = 9.3 Hz, *H*<sub>Ar</sub>), 2.03-1.85 (4H, m, *H*<sub>Bu</sub>), 1.05-0.94 (4H, m, *H*<sub>Bu</sub>), 0.58 (6H, t, *J* = 7.3 Hz, *H*<sub>Bu</sub>), 0.55-0.39 (4H, m, *H*<sub>Bu</sub>). **<sup>13</sup>C{<sup>1</sup>H} NMR** (100 MHz, CDCl<sub>3</sub>): δ = 168.6, 164.5, 153.8, 152.6, 152.5, 148.3, 147.3, 147.2, 144.6, 138.6, 132.7, 132.0, 131.1, 130.5, 130.2, 129.5, 129.4, 127.0, 126.8, 126.1, 125.2, 124.9, 124.4, 123.8, 122.1, 122.0, 121.3, 121.1, 118.1, 115.6, 113.7, 112.8, 112.7, 111.9, 91.9, 89.4, 85.2, 78.5, 55.8, 39.8, 26.0, 23.0, 13.9. **IR** (KBr, cm<sup>-1</sup>): ν = 3036 (m, C<sub>Ar</sub>-H), 2928 (m, C<sub>Ar</sub>-H), 2221 (m, C≡N), 2195 (vw, C≡C), 1606 (s, C=C), 1586 (s, C=C<sub>Ar</sub>). **Raman** (neat, cm<sup>-1</sup>): ν = 3065 (vw, C<sub>Ar</sub>-H), 2222 (s, C≡N), 2199 (s, C≡C), 1609 (vs, C=C), 1523 (s, C=C<sub>Ar</sub>). **HRMS**: calculated for C<sub>67</sub>H<sub>53</sub>N<sub>6</sub> [M+H]<sup>+</sup> 941.43262, found 941.4325, calculated for C<sub>67</sub>H<sub>52</sub>N<sub>6</sub> M<sup>+</sup> 940.42535, found 940.4258. **UV-vis** (CH<sub>2</sub>Cl<sub>2</sub>): λ<sub>max</sub> (log ε) = 293 (4.60), 348 (4.64), 409 (4.66), 483 (4.66) nm.

**Synthesis of compound 3**: A solution of the fluorene derivative **6** (65 mg, 0.091 mmol) and TCNE (12 mg, 0.091 mmol) in CH<sub>2</sub>Cl<sub>2</sub> (0.9 mL) was stirred at 20 °C for 16 h. The reaction mixture was purified by column chromatography [Petroleum ether/Et<sub>2</sub>O (1:0) to (3:2)] to give the title compound (73 mg, 95%) as a dark fushia solid. **MP**: 108-110 °C. **R<sub>f</sub>**: 0.20 [Petroleum ether/Et<sub>2</sub>O (4:1)]. **<sup>1</sup>H NMR** (400 MHz, CDCl<sub>3</sub>): δ = 7.92 (1H, d, *J* = 1.5 Hz, *H*<sub>Flu</sub>), 7.75 (2H, d, *J* = 9.2 Hz, *H*<sub>Ar</sub>), 7.71 (1H, d, *J* = 8.2 Hz, *H*<sub>Flu</sub>), 7.65-7.57 (2H, m, 2*H*<sub>Flu</sub>), 7.43 (4H, t, *J* = 7.8 Hz, *H*<sub>Ar</sub>), 7.37-7.24 (10H, m, 2*H*<sub>Ar</sub> and *H*<sub>Flu</sub>), 7.20 (4H, d, *J* = 7.6 Hz, *H*<sub>Ar</sub>), 7.14 (3H, m, 2*H*<sub>Ar</sub>), 7.12-7.05 (1H, m, *H*<sub>Flu</sub>), 7.00 (2H, d, *J* = 9.2 Hz, *H*<sub>Ar</sub>), 2.07-1.83 (4H, m, *H*<sub>Bu</sub>), 1.19-1.06 (4H, m, *H*<sub>Bu</sub>), 0.75 (6H, t, *J* 7.3 Hz, *H*<sub>Bu</sub>), 0.72-0.63 (4H, m, *H*<sub>Bu</sub>). **<sup>13</sup>C{<sup>1</sup>H} NMR** (100 MHz, CDCl<sub>3</sub>): δ = 168.3, 165.0, 154.3, 153.7, 151.9, 150.0, 148.3, 147.4, 144.6, 132.9, 132.0, 130.2, 129.8, 129.5, 129.1, 127.0, 126.7, 125.0, 124.1, 123.8, 122.2, 122.1, 120.0, 118.1, 117.2, 113.8, 113.1, 112.8, 112.2, 83.4, 78.6, 55.5, 39.6, 26.1, 22.9, 13.9. **IR**

(KBr,  $\text{cm}^{-1}$ ):  $\nu = 3036$  (m,  $\text{C}_{\text{Ar}}\text{-H}$ ),  $2928$  (m,  $\text{C}_{\text{Ar}}\text{-H}$ ),  $2221$  (vw,  $\text{C}\equiv\text{N}$ ),  $1605$  (s,  $\text{C}=\text{C}$ ),  $1587$  (s,  $\text{C}=\text{C}_{\text{Ar}}$ ). **Raman** (neat,  $\text{cm}^{-1}$ ):  $\nu = 3065$  (vw,  $\text{C}_{\text{Ar}}\text{-H}$ ),  $2223$  (s,  $\text{C}\equiv\text{N}$ ),  $1603$  (s,  $\text{C}=\text{C}$ ),  $1522$  (vs,  $\text{C}=\text{C}_{\text{Ar}}$ ). **HRMS**: calculated for  $\text{C}_{59}\text{H}_{49}\text{N}_6$   $[\text{M}+\text{H}]^+$   $841.40187$ , found  $841.4011$ , calculated for  $\text{C}_{47}\text{H}_{39}\text{N}_5$   $\text{M}^+$   $840.39405$ , found  $840.3942$ . **UV-vis** ( $\text{CH}_2\text{Cl}_2$ ):  $\lambda_{\text{max}}$  ( $\log \epsilon$ ) =  $306$  (4.54),  $417$  sh (4.44),  $512$  (4.62) nm.

**Synthesis of 2-(4-diphenylamino-1-phenylethynyl)-9,9-dibutyl-fluorene (4):** To a flask under argon were added 2-bromo-9,9-dibutylfluorene (**8**; 1.05 g, 2.99 mmol, 1 eq.), *N*-(4-phenylethynyl)-*N,N*-diphenylamine (**7**; 0.87 g, 3.23 mmol, 1.1 eq.), CuI (27 mg, 0.15 mmol, 0.05 eq.), and Pd(PPh<sub>3</sub>)<sub>2</sub>Cl<sub>2</sub> (105 mg, 0.15 mmol, 0.05 eq.). Toluene (20 mL) and diisopropylamine (5 mL) were subsequently added. The colour of the reaction medium changed from orange to black. After stirring 12 h at 25 °C, the solvents were evaporated and the resulting dark solid was dissolved in CH<sub>2</sub>Cl<sub>2</sub> (20 mL) and passed through a Celite pad. After evaporation of the solvent, the solid was washed with water and brine, dried in vacuum, and purified by flash chromatography using hexane/CH<sub>2</sub>Cl<sub>2</sub> (7:3) mixtures, to afford the title compound as a pale yellow solid (1.372 g, 52%). **MP**: 141-142 °C. **R<sub>f</sub>**: 0.44 [hexane/CH<sub>2</sub>Cl<sub>2</sub> (7:3)]. **<sup>1</sup>H-NMR** (400 MHz, CDCl<sub>3</sub>):  $\delta = 7.68\text{-}7.77$  (m, 2H,  $H_{\text{Ar}}$ ),  $7.48$  (d,  $J = 8.4$  Hz, 2H,  $H_{\text{Ar}}$ ),  $7.56$  (m, 2H,  $H_{\text{Ar}}$ ),  $7.29\text{-}7.42$  (m, 7H,  $H_{\text{Ar}}$ ),  $7.19$  (d,  $J = 7.9$  Hz, 4H,  $H_{\text{Ar}}$ ),  $7.1$  (m, 4H,  $H_{\text{Ar}}$ ),  $2.04$  (t,  $J = 8.2$  Hz, 4H,  $H_{\text{Bu}}$ ),  $1.05\text{-}1.22$  (m, 4H,  $H_{\text{Bu}}$ ),  $0.73$  (t,  $J = 7.3$  Hz, 6H,  $H_{\text{Bu}}$ ),  $0.60\text{-}0.90$  (m, 4H,  $H_{\text{Bu}}$ ). **<sup>13</sup>C{<sup>1</sup>H}-NMR** (100 MHz, CDCl<sub>3</sub>):  $\delta = 151.0, 150.7, 147.9, 147.3, 141.2, 140.5, 132.5, 130.5, 129.4, 127.4, 126.9, 125.8, 125.0, 123.5, 122.9, 122.4, 121.8, 119.9, 119.6, 116.3, 89.8, 89.7, 55.1, 40.2, 25.9, 23.1, 13.8$ . **IR** (KBr,  $\text{cm}^{-1}$ ):  $\nu = 3036$  (m,  $\text{C}_{\text{Ar}}\text{-H}$ ),  $2925$  (m,  $\text{C}_{\text{Ar}}\text{-H}$ ),  $2197$  (vw,  $\text{C}\equiv\text{C}$ ),  $1590$  (s,  $\text{C}=\text{C}_{\text{Ar}}$ ). **Raman** (neat,  $\text{cm}^{-1}$ ):  $\nu = 2200$  (s,  $\text{C}\equiv\text{C}$ ),  $1620$  (vs,  $\text{C}=\text{C}_{\text{Ar}}$ ). **HRMS**: calc. for  $\text{C}_{41}\text{H}_{39}\text{N}$ :  $545.3083$   $[\text{M}]^+$ , found  $545.3087$ . **UV-vis** ( $\text{CH}_2\text{Cl}_2$ ):  $\lambda_{\text{max}}$  ( $\log \epsilon$ ) =  $302$  (4.51),  $324$  (4.47),  $365$  (4.74).

**Synthesis of 2,7-bis(4-diphenylamino-1-phenylethynyl)-9,9-dibutyl-fluorene (5):** To a flask under argon were added 2,7-diodo-9,9-dibutylfluorene (**9**; 1.22 g, 2.30 mmol, 1 eq.), *N*-(4-phenylethynyl)-*N,N*-diphenylamine (**7**, 1.36 g, 5.06 mmol, 2.2 eq.), CuI (21.8 mg, 0.115 mmol, 0.05 eq.), and Pd(PPh<sub>3</sub>)<sub>2</sub>Cl<sub>2</sub> (81 mg, 0.115 mmol, 0.05 eq.). Toluene (20 mL)

and diisopropylamine (5 mL) were subsequently added. The colour of the reaction medium changed from orange to orange-brown. After stirring 1 h at 25 °C, an orange precipitate was formed. The mixture was further heated 12 h at 80 °C. Solvents were evaporated and the remaining solid was dissolved in CH<sub>2</sub>Cl<sub>2</sub> (20 mL) and passed through a short plug of Celite before being washed with a saturated solution of NH<sub>4</sub>Cl and with brine. After drying and evaporation, the resulting yellow solid was purified by flash chromatography using hexane/CH<sub>2</sub>Cl<sub>2</sub> (8:2) mixtures, providing the title compound as a golden yellow solid (1.435 g, 77%). **MP**: 273-275 °C (Dec). **R<sub>f</sub>**: 0.30 (hexane/CH<sub>2</sub>Cl<sub>2</sub> [8:2]). **<sup>1</sup>H-NMR** (400 MHz, CDCl<sub>3</sub>): δ = 7.65 (d, *J* = 7.7 Hz, 2H, *H*<sub>Ar</sub>), 7.46-7.53 (m, 4H, *H*<sub>Ar</sub>), 7.41 (d, *J* = 7.9 Hz, 4H, *H*<sub>Ar</sub>), 7.32-7.23 (m, 8H, *H*<sub>Ar</sub>), 7.13 (d, *J* = 7.9 Hz, 8H, *H*<sub>Ar</sub>), 6.96-7.10 (m, 8H, *H*<sub>Ar</sub>), 1.82-2.06 (m, 4H, *H*<sub>Bu</sub>), 1.00-1.15 (m, 4H, *H*<sub>Bu</sub>), 0.68 (t, *J* = 7.2 Hz, 6H, *H*<sub>Bu</sub>), 0.5-0.65 (m, 4H, *H*<sub>Bu</sub>). **<sup>13</sup>C{<sup>1</sup>H}-NMR** (100 MHz, CDCl<sub>3</sub>): δ = 151.1, 147.9, 147.2, 140.5, 132.5, 130.6, 129.4, 125.8, 125.0, 123.6, 122.3, 122.2, 119.9, 116.2, 90.1, 89.7, 55.1, 40.3, 25.9, 23.1, 13.9. **HRMS**: calc. for C<sub>61</sub>H<sub>52</sub>N<sub>2</sub>: 812.4130 [M]<sup>+</sup>, found 812.4140. **IR** (KBr, cm<sup>-1</sup>): ν = 3034 (m, C<sub>Ar</sub>-H), 2927 (m, C<sub>Ar</sub>-H), 2194 (vw, C≡C), 1590 (s, C<sub>Ar</sub>=C<sub>Ar</sub>). **Raman** (neat, cm<sup>-1</sup>): ν = 2197 (s, C≡C), 1608 (vs, C=C<sub>Ar</sub>). **UV-vis** (CH<sub>2</sub>Cl<sub>2</sub>): λ<sub>max</sub> (log ε) = 301 (4.74), 390 (5.10).

**Synthesis of 2-(4-diphenylamino-1-phenylethynyl)-7-diphenylamino-9,9-dibutylfluorene (6)**: To a flask under argon were added 2-iodo-7-diphenylamino-9,9-dibutylfluorene (**10**; 0.735 g, 1.28 mmol, 1 eq.), *N*-(4-phenylethynyl)-*N,N*-diphenylamine (**7**, 0.414 g, 1.54 mmol, 1.2 eq.), CuI (12 mg, 0.64 mmol, 0.05 eq.), and Pd(PPh<sub>3</sub>)<sub>2</sub>Cl<sub>2</sub> (45 mg, 0.64 mmol, 0.05 eq.). Toluene (20 mL) and diisopropylamine (5 mL) were subsequently added. The colour of the reaction medium changed from orange to brown. After stirring 12 h at 60 °C, the solvents were evaporated and the resulting dark brown solid was dissolved in CH<sub>2</sub>Cl<sub>2</sub> (20 mL) and passed through a Celite pad. After evaporation of the solvent, the solid was washed with water and brine, dried in vacuum, and purified by flash chromatography using hexane/CH<sub>2</sub>Cl<sub>2</sub> (7:3) mixtures to afford the title compound, as a yellow solid (0.671 g, 73%). **MP**: 217-218 °C (Dec). **R<sub>f</sub>**: 0.32 (hexane/CH<sub>2</sub>Cl<sub>2</sub> [7:3]). **<sup>1</sup>H-NMR** (400 MHz, CDCl<sub>3</sub>): δ = 7.56 (t, *J* = 8.5 Hz, 2H, *H*<sub>Ar</sub>), 7.49-7.36 (m, 4H, *H*<sub>Ar</sub>), 7.32-7.21 (m, 12H, *H*<sub>Ar</sub>), 7.16-6.93 (m, 16H, *H*<sub>Ar</sub>), 1.94-1.78

(m, 4H,  $H_{Bu}$ ), 1.15-1.01 (m, 4H,  $H_{Bu}$ ), 0.71 (t,  $J = 7.3$  Hz, 6H,  $H_{Bu}$ ), 0.68-0.55 (m, 4H,  $H_{Bu}$ ).  $^{13}\text{C}\{^1\text{H}\}$ -NMR (100 MHz,  $\text{CDCl}_3$ ):  $\delta = 152.5, 150.6, 147.9, 147.8, 147.5, 147.3, 141.0, 135.6, 133.4, 132.5, 130.6, 129.5, 129.4, 129.2, 125.7, 125.3, 125.0, 124.0, 123.5, 123.4, 122.7, 122.4, 121.6, 120.9, 120.6, 119.1, 119.0, 116.4, 89.9, 89.5, 55.0, 40.0, 26.0, 23.0, 13.9$ . **HRMS**: calc. for  $\text{C}_{53}\text{H}_{48}\text{N}_2$ : 712.3817  $[\text{M}]^+$ , found 712.3820. **IR** (KBr,  $\text{cm}^{-1}$ ):  $\nu = 3033$  (m,  $\text{C}_{Ar}\text{-H}$ ), 2927 (m,  $\text{C}_{Ar}\text{-H}$ ), 2197 (vw,  $\text{C}\equiv\text{C}$ ), 1590 (s,  $\text{C}=\text{C}_{Ar}$ ). **Raman** (neat,  $\text{cm}^{-1}$ ):  $\nu = 2202$  (s,  $\text{C}\equiv\text{C}$ ), 1603 (vs,  $\text{C}=\text{C}_{Ar}$ ). **UV-vis** ( $\text{CH}_2\text{Cl}_2$ ):  $\lambda_{\text{max}}$  ( $\log \epsilon$ ) = 301 (4.55), 385 (4.92).

**Synthesis of 2-iodo-7-diphenylamino-9,9-dibutylfluorene (10)**: Metallic Cu (0.65g, 10.4 mmol, 1.1 eq.) was activated by vigorous stirring in a 2% solution of  $\text{I}_2$  in acetone for 15-20 min, followed by stirring in an acidic (30% HCl) acetone solution for 20 min before being separated and dried under vacuum. This sample was subsequently mixed (in the solid state) with 2,7-diodo-9,9-dibutylfluorene (**9**; 5.00 g, 9.4 mmol, 1 eq.), diphenylamine (1.56 g, 9.4 mmol, 1 eq.),  $\text{K}_2\text{CO}_3$  (3.77g, 27.4 mmol, 2.9 eq.), and 18-crown-6 (0.62 g, 2.0 mmol, 0.25 eq.) in deoxygenated 1,2-dichlorobenzene and heated to 175 °C for 48 h. The reaction mixture was then filtered through a Celite plug and washed with a saturated solution of  $\text{NH}_4\text{Cl}$  until the washings remained colourless. The suspension was then filtered and the solvent evaporated. After drying, the title compound was obtained after purification by flash chromatography, eluting with hexane/ $\text{CH}_2\text{Cl}_2$  (9:1) mixtures, as a tan solid (0.776 g, 15%). **MP**: 122-123 °C. **R<sub>f</sub>**: 0.38 (hexane/ $\text{CH}_2\text{Cl}_2$  [9:1]).  $^1\text{H}$ -NMR (400 MHz,  $\text{CDCl}_3$ ):  $\delta = 7.61$ -7.67 (m, 2H,  $H_{Ar}$ ), 7.56 (d,  $J = 8.2$  Hz, 1H,  $H_{Ar}$ ), 7.39 (d,  $J = 8.3$  Hz, 1H,  $H_{Ar}$ ), 7.29 ( $t^3$ ,  $J = 7.7$  Hz, 4H,  $H_{Ph}$ ), 7.22-7.10 (m, 5H,  $H_{Ar}$ ), 7.08-7.02 (m, 3H,  $H_{Ar}$ ), 1.87 (m, 4H,  $H_{Bu}$ ), 1.04-1.19 (m, 4H,  $H_{Bu}$ ), 0.75 (t,  $J = 7.3$  Hz, 6H,  $H_{Bu}$ ), 0.61-0.71 (m, 4H,  $H_{Bu}$ ).  $^{13}\text{C}\{^1\text{H}\}$ -NMR (125 MHz,  $\text{CDCl}_3$ ):  $\delta = 153.6, 152.1, 148.04, 148.3, 141.1, 136.4, 135.6, 132.4, 129.8, 124.6, 123.8, 123.3, 121.4, 121.1, 119.4, 92.2, 55.7, 40.5, 26.6, 23.6, 14.5$ . **HRMS**: calc. for  $\text{C}_{33}\text{H}_{34}\text{N}_1\text{I}_1$ : 571.1730  $[\text{M}]^+$ , found 571.1730. **IR** (KBr,  $\text{cm}^{-1}$ ):  $\nu = 1611$  (m,  $\text{C}=\text{C}_{Flu}$ ), 1596, 1488 (vs,  $\text{C}=\text{C}_{NPh2}$ ). **Raman** (neat,  $\text{cm}^{-1}$ ):  $\nu = 1614$  (s,  $\text{C}=\text{C}_{Flu}$ ), 1593 (vs,  $\text{C}=\text{C}_{NPh2}$ ).



**Luminescence measurements.** Luminescence measurements in solution were performed in dilute air-saturated solutions contained in quartz cells of 1 cm pathlength (*ca.*  $10^{-6}$  M, optical density  $< 0.1$ ) at room temperature (298 K), using an Edinburgh Instruments (FLS920) fluorimeter equipped with a 450 W Xenon lamp and a Peltier-cooled Hamamatsu R928P photomultiplier tube in photon-counting mode. Fully corrected emission spectra were obtained at  $\lambda_{\text{ex}} = \lambda_{\text{max}}^{\text{abs}}$  with an optical density at  $\lambda_{\text{ex}} \leq 0.1$  to minimize internal absorption. Luminescence quantum yields were measured according to literature procedures.<sup>[37,38]</sup> UV-vis absorption spectra used for the calculation of the luminescence quantum yields were recorded using a double-beam Jasco V-570 spectrometer. Luminescence lifetimes were measured by time-correlated single photon counting (TCSPC). Excitation was achieved by a hydrogen-filled nanosecond flashlamp (repetition rate 40 kHz) or a pulsed diode laser EPL-440. The instrument response (FWHM *ca.* 1 ns) was determined by measuring the light scattered by a Ludox suspension. The TCSPC traces were analyzed by standard iterative reconvolution methods implemented in the software of the fluorimeter. Sucrose octaacetate (SOA) was purchased from Acros and purified according to lit.<sup>[23]</sup> The SOA glass samples were prepared by typically adding 15  $\mu\text{L}$  of  $5 \cdot 10^{-4}$  M TCBD stock solution in  $\text{CH}_2\text{Cl}_2$  to 3 g of melted SOA in a test tube. The mixture was homogenized, poured into a quartz fluorescence cell (1 cm  $\times$  1 cm pathlength), and allowed to cool down to room temperature. .

**Two-photon excited fluorescence measurements.** 2PA cross sections ( $\sigma_2$ ) of compounds **4-6** were derived from the two-photon excited fluorescence (TPEF) cross sections ( $\sigma_2 \Phi_{\text{F}}$ ) and the fluorescence emission quantum yield ( $\Phi_{\text{F}}$ ). TPEF cross sections were measured relative to fluorescein in 0.01 M aqueous NaOH<sup>[39]</sup> using the well-established method described by Xu and Webb<sup>[40]</sup> and the appropriate solvent-related refractive index corrections.<sup>[41]</sup> Reference values between 700 and 715 nm for fluorescein were taken from literature.<sup>[10e]</sup> The quadratic dependence of the fluorescence intensity on the excitation power was checked for each sample and all wavelengths. Measurements were conducted using an excitation source delivering fs pulses. A Chameleon Ultra II (Coherent) was used generating

140 fs pulses at 80 MHz repetition rate. The excitation was focused into the cuvette through a microscope objective (10X, NA 0.25). The fluorescence was detected in epifluorescence mode via a dichroic mirror (Chroma 675dcxru) and a barrier filter (Chroma e650sp-2p) by a compact CCD spectrometer module BWTek BTC112E. Total fluorescence intensities were obtained by integrating the corrected emission. .

**Z-scan Studies on 1-3.** Third-order nonlinear optical properties were investigated with an amplified femtosecond laser system using a Clark-MXR CPA-2001 Ti-sapphire regenerative amplifier to pump a Light Conversion TOPAS optical parametric amplifier. Experiments were performed over a wide range of wavelengths using different modes of the OPA output and employing polarizing optics, spatial filtering and colour glass filters to reject unwanted wavelengths. The pulse duration was approximately 150 fs and the repetition rate was 250 Hz. The pulse energy was adjusted to keep the nonlinear phase shifts that were obtained from the samples in the range of roughly 0.3 -1.5 rad, which typically corresponded to light intensities of the order of 100 GW/cm<sup>2</sup>. Solutions of the compounds in dichloromethane of *ca.* 0.5 w/w% concentration were placed in 1 mm stoppered Starna glass cells. An identical cell was used for measurements of Z-scans on pure solvent. All measurements were calibrated by referencing to signals obtained from a 3 mm thick fused silica plate, and the NLO properties of the solute were determined as described previously.<sup>[42]</sup>

**Computational Details.** Gas phase geometry optimizations of **1-6** were performed by DFT on simplified (**C1-C6**) models (for reasons of computational expediency) where the butyl chains on the fluorene groups have been replaced by methyls. The Gaussian 09 program package (Revision D.01)<sup>[43]</sup> was used and the hybrid functional PBE1 which uses 25% exchange and 75% correlation weighting was employed.<sup>[44]</sup> This functional has been shown to give very good results in the case of magnetic, vibrational, and electronic properties of molecules, compared to DFT functionals that include extensive parameterization.<sup>[45]</sup> In all calculations and for all atoms, all-electron Slater-type orbital basis sets were used (6-31(p))

which includes only polarization function on the heavy atoms. UV-Vis spectra were calculated using time-dependent methods (TD-DFT).<sup>[46]</sup>

## Acknowledgements

The CNRS and the “Région Bretagne” (ARED) are acknowledged for financial support to N.R, and the Erasmus program and UR1 for financial support to Z.P. A. Bondon (RMN-ILP/UMR 6226) is acknowledged for experimental assistance. M.B. thanks the "Région Bretagne" for a post-doctoral fellowship. K.M. J.O.B. & M.S. acknowledge financing by NCN Maestro grant (DEC-2013/10/A/ST4/00114). M. G. H. thanks the Australian Research Council for support. The support of the Wroclaw Centre for Networking and Supercomputing is also acknowledged.

## References

- [1] a) M. Betou, N. Kerisit, E. Meledje, Y. R. Leroux, C. Katan, J.-F. Halet, J.-C. Guillemin, Y. Trolez, *Chem. Eur. J.* **2014**, *20*, 9553-9557; b) T. Shoji, E. Shimomura, M. Maruyama, A. Maruyama, S. Ito, T. Okujima, K. Toyota, N. Morita, *Eur. J. Org. Chem.* **2013**, 7785–7799; c) R. Misra, P. Gautam, S. M. Mobin, *J. Org. Chem.* **2013**, *78*, 12440–12452; d) R. Garcia, M. A. Herranz, M. R. Torres, P.-A. Bouit, J. L. Delgado, J. Calbo, P. M. Viruela, E. Ortí, N. Martín, *J. Org. Chem.* **2012**, *77*, 10707-10717; e) D. Koszelewski, A. Nowak-Król, D. T. Gryko, *Chem. Asian J.* **2012**, *7*, 1887-1894; f) T. Shoji, J. Higashi, S. Ito, T. Okujima, M. Yasunami, N. Morita, *Chem. Eur. J.* **2011**, *17*, 5116-5129; g) X. Tang, W. Liu, J. Wu, C.-S. Lee, J. You, P. Wang, *J. Org. Chem.* **2010**, *75*, 7273-7278; h) S.-I. Kato, M. Kivala, W. B. Schweizer, C. Boudon, J.-P. Gisselbrecht, F. Diederich, *Chem. Eur. J.* **2009**, *15*, 8687-8691; i) T. Shoji, S. Ito, K. Toyota, M. Yasunami, N. Morita, *Chem. Eur. J.* **2008**, *14*, 8398-8408; j) Y. Morioka, N. Yoshizawa, J.-I. Nishida, Y. Yamashita, *Chem. Lett.* **2004**, *33*, 1190-1191; k) T.

## Full Paper

- Mochida, S. Yamazaki, *J. Chem. Soc. Dalton Trans.* **2002**, 3559-3564; l) X. Wu, J. Wu, Y. Liu, A. K.-Y. Jen, *J. Am. Chem. Soc.* **1999**, *121*, 472-473.
- [2] C. Cai, I. Liakatas, M.-S. Wong, M. Bösch, C. Bosshard, P. Günter, S. Concilio, N. Tirelli, U. W. Suter, *Org. Lett.* **1999**, *1*, 1847-1849.
- [3] a) J. C. May, I. Biaggio, F. Bures, F. Diederich, *Appl. Phys. Lett.* **2007**, *90*, 251106/251101-251103; b) J. C. May, J. H. Lim, I. Biaggio, N. P. Moonen, T. Michinobu, F. Diederich, *Opt. Lett.* **2005**, *30*, 3057-3059; c) T. Michinobu, J. C. May, J. H. Lim, C. Boudon, J.-P. Gisselbrecht, P. Seiler, M. Gross, I. Biaggio, F. Diederich, *Chem. Commun.* **2005**, 737-739.
- [4] a) S.-I. Kato, F. Diederich, *Chem. Commun.* **2010**, *46*, 1994-2006; b) M. Kivala, F. Diederich, *Acc. Chem. Res.* **2009**, *42*, 235-248.
- [5] B. Esembeson, M. L. Scimeca, T. Michinobu, F. Diederich, I. Biaggio, *Adv. Mater.* **2008**, *20*, 4584-4587.
- [6] M. T. Beels, M. S. Fleischman, I. Biaggio, B. Breiten, M. Jordan, F. Diederich, *Opt. Mater. Express* **2012**, *2*, 294-303.
- [7] a) N. P. Moonen, R. Gist, C. Boudon, J.-P. Gisselbrecht, P. Seiler, T. Kawai, A. Kishioka, M. Gross, M. Irie, F. Diederich, *Org. Biomol. Chem.* **2003**, *1*, 2032-2034; b) G. S. He, L.-S. Tan, Q. Zheng, P. N. Prasad, *Chem. Rev.* **2008**, *108*, 1245-1330.
- [8] F. Z. Henari, *J. Opt. A: Pure Appl. Opt.* **2001**, *3*, 188-190.
- [9] a) M. Pawlicki, H. A. Collins, R. G. Denning, H. L. Anderson, *Angew. Chem. Int. Ed.* **2009**, *48*, 3244-3266; b) H. M. Kim, B. R. Cho, *Chem. Commun.* **2009**, 153-164.
- [10] a) A. Rebane, M. Drobizhev, N. S. Makarov, E. Beuerman, J. E. Haley, D. M. Krein, A. R. Burke, J. L. Flikkema, T. M. Cooper, *J. Phys. Chem. A* **2011**, *115*, 4255-4262; b) F. Terenziani, C. Katan, E. Badaeva, S. Tretiak, M. Blanchard-Desce, *Adv. Mater.* **2008**, *20*, 4541-4678; c) O. Mongin, L. Porrès, M. Charlot, C. Katan, M. Blanchard-Desce, *Chem. Eur. J.* **2007**, *13*, 1481-1498; d) C.-Y. Chen, Y. Tang, Y.-J. Cheng, A. C. Young,

- J.-W. Ka, A. K.-Y. Jen, *J. Am. Chem. Soc.* **2007**, *129*, 7220-7221; e) C. Katan, S. Tretiak, M. H. V. Werts, A. J. Bain, R. J. Marsh, N. Leonczek, N. Nicolaou, E. Badaeva, O. Mongin, M. Blanchard-Desce, *J. Phys. Chem. B* **2007**, *111*, 9468-9483; f) O. Mongin, T. R. Krishna, M. H. V. Werts, A.-M. Caminade, J.-P. Majoral, M. Blanchard-Desce, *Chem. Commun.* **2006**, 915–917.
- [11] N. I. Nijegorodov, W. S. Downey, *J. Phys. Chem.* **1994**, *98*, 5639-5643.
- [12] C. Rouxel, M. Charlot, O. Mongin, T. R. Krishna, A.-M. Caminade, J.-P. Majoral, M. Blanchard-Desce, *Chem. Eur. J.* **2012**, *18*, 16450-16462.
- [13] a) T. Michinobu, C. Boudon, J.-P. Gisselbrecht, P. Seiler, B. Frank, N. N. P. Moonen, M. Gross, F. Diederich, *Chem. Eur. J.* **2006**, *12*, 1889-1905; b) F. Tancini, F. Monti, K. Howes, A. Belbakra, A. Listorti, W. B. Schweizer, P. Reutenauer, J.-L. Alonso-Gomez, C. Chiorboli, L. M. Uerner, J.-P. Gisselbrecht, C. Boudon, N. Armaroli, F. Diederich, *Chem. Eur. J.* **2014**, *20*, 202-216; c) F. Monti, A. Venturini, A. Nenov, F. Tancini, A. D. Finke, F. Diederich, N. Armaroli, *J. Phys. Chem. A* **2015**, *119*, 10677-10683.
- [14] a) X. Yang, Y. Zhao, X. Zhang, R. Li, J. Dang, Y. Li, G. Zhou, Z. Wu, D. Ma, W.-Y. Wong, X. Zhao, A. Ren, L. Wang, X. Hou, *J. Mater. Chem.* **2012**, *22*, 7136-7148; b) C. Cheng, W. Wu, H. Guo, S. Ji, P. Song, K. Han, J. Zhao, X. Zhang, Y. Wu, G. Du, *Eur. J. Inorg. Chem.* **2010**, 4683-4696.
- [15] a) F. Malvotti, C. Rouxel, O. Mongin, P. Hapiot, L. Toupet, M. Blanchard-Desce, F. Paul, *Dalton Trans.* **2011**, *40*, 6616-6618; b) F. Paul, *work in progress*.
- [16] K. D. Belfield, M. V. Bondar, *J. Phys. Org. Chem.* **2003**, *16*, 194–201.
- [17] G. Grelaud, M. P. Cifuentes, T. Schwich, G. Argouarch, S. Petrie, R. Stranger, F. Paul, M. G. Humphrey, *Eur. J. Inorg. Chem.* **2012**, 65–75.
- [18] A. Weller, *Z. Phys. Chem. N. F.* **1982**, *133*, 93-98.
- [19] In this equation,  $e$  is the electron charge,  $\epsilon_0$  is the dielectric constant in vacuum,  $\epsilon$  is the relative dielectric constant and  $a$  is the distance between the positive and negative

charge in the CT state. Based on the computed HOMO and LUMO for each compound, the later was obtained by considering the distance between the most electronegative nitrogen atom and midpoint of the nearby TCBD unit.

- [20] D. Cao, Z. Liu, Y. Deng, G. Li, G. Zhang, *Dyes and Pigments* **2009**, *83*, 348–353.
- [21] A. M. Brouwer, *Pure Appl. Chem.* **1980**, *83*, 2213-2228.
- [22] a) B. Valeur, *Molecular Fluorescence: Principles and Applications*, Wiley-VCH Verlag GmbH, Weinheim, **2001**; b) W. Rettig, *Angew. Chem.* **1986**, *98*, 636-986.
- [23] G. Jones, II, D. Yan, J. Hu, J. Wan, B. Xia, V. I. Vullev, *J. Phys. Chem. B* **2007**, *111*, 6921-6929.
- [24] Q. Bellier, N. S. Makarov, P.-A. Bouit, S. Rigaut, K. Kamada, P. Feneyrou, G. Berginc, O. Maury, J. W. Perry, C. Andraud, *Phys. Chem. Chem. Phys.* **2012**, *14*, 15299–15307.
- [25] M. G. Kuzyk, *J. Chem. Phys.* **2003**, *119*, 8327-8334.
- [26] M. G. Kuzyk, *J. Mater. Chem.* **2009**, *19*, 7444-7465.
- [27] Similar 2PA cross-sections were determined from TPEF and Z-scan for **4**, validating the comparison between 2PA values determined by different methods for both sets of compounds.
- [28] J. M. Hales, J. Matichak, S. Barlow, S. Ohira, K. Yesudas, J.-L. Brédas, J. W. Perry, S. R. Marder, *Science* **2010**, *327*, 1485-1488.
- [29] T. Jadhav, R. Maragani, R. Misra, V. Sreeramulu, D. N. Rao, S. M. Mobin, *Dalton Trans.* **2013**, *42*, 4340-4342.
- [30] G. Grelaud, M. P. Cifuentes, F. Paul, M. G. Humphrey, *J. Organomet. Chem.* **2014**, *751*, 181-200 (150th Anniversary Special Issue).
- [31] J. P. Merrick, D. Moran, L. Radom, *J. Phys. Chem. A* **2007**, *111*, 11683-11700.
- [32] C. Adamo, D. Jacquemin, *Chem. Soc. Rev.* **2013**, *42*, 845-856 and refs therein.

## Full Paper

- [33] D. F. Shriver, M. A. Drezdson, *The Manipulation of Air-Sensitive Compounds*, Wiley and sons, New-York, **1986**.
- [34] F. Xu, L. Peng, A. Orita, J. Otera, *Org. Lett.* **2012**, *14*, 3970–3973.
- [35] a) D. Li, H. Li, M. Liu, J. Chen, J. Ding, X. Huang, H. Wu, *Macromol. Chem. Phys.* **2014**, *215*, 82-89; b) F. Li, Z. Chen, W. Wei, H. Cao, Q. Gong, F. Teng, L. Qian, Y. Wang, *J. Phys. D: Appl. Phys.* **2004**, *37*, 1613–1616.
- [36] N. G. Connelly, W. E. Geiger, *Chem. Rev.* **1996**, *96*, 877-910.
- [37] N. Demas, G. A. Crosby, *J. Phys. Chem.* **1971** *75*, 991-1024.
- [38] D. F. Eaton, *Pure Appl. Chem.* **1988**, *60*, 1107-1114.
- [39] M. A. Albota, C. Xu, W. W. Webb, *Appl. Opt.* **1998**, *37*, 7352-7356.
- [40] C. Xu, W. W. Webb, *J. Opt. Soc. Am. B* **1996**, *13*, 481-491.
- [41] M. H. V. Werts, N. Nerambourg, D. Pélégruy, Y. Le Grand, M. Blanchard-Desce, *Photochem. Photobiol. Sci.* **2005**, *4*, 531-538.
- [42] a) M. Samoc, A. Samoc, G. T. Dalton, M. P. Cifuentes, M. G. Humphrey, P. A. Fleitz, in *Multiphoton Processes in Organics and Their Application* (Eds.: I. Rau, F. Kajzar), Old City Publishing, Philadelphia, **2011**, pp. 341-355; b) B. Babgi, L. Rigamonti, M. P. Cifuentes, T. C. Corkery, M. D. Randles, T. Schwich, S. Petrie, R. Stranger, A. Teshome, I. Asselberghs, K. Clays, M. Samoc, M. G. Humphrey, *J. Am. Chem. Soc.* **2009**, *131*, 10293–10307.
- [43] M. J. Frisch, G. W. Trucks, H. B. Schlegel, G. E. Scuseria, M. A. Robb, J. R. Cheeseman, G. Scalmani, V. Barone, B. Mennucci, G. A. Petersson, H. Nakatsuji, M. Caricato, X. Li, H. P. Hratchian, A. F. Izmaylov, J. Bloino, G. Zheng, J. L. Sonnenberg, M. Hada, M. Ehara, K. Toyota, R. Fukuda, J. Hasegawa, M. Ishida, T. Nakajima, Y. Honda, O. Kitao, H. Nakai, T. Vreven, J. A. Montgomery (Jr.), J. E. Peralta, F. Ogliaro, M. Bearpark, J. J. Heyd, E. Brothers, K. N. Kudin, V. N. Staroverov, R. Kobayashi, J. Normand, K. Raghavachari, A. Rendell, J. C. Burant, S. S. Iyengar, J. Tomasi, M.

## Full Paper

Cossi, N. Rega, N. J. Millam, M. Klene, J. E. Knox, J. B. Cross, V. Bakken, C. Adamo, J. Jaramillo, R. Gomperts, R. E. Stratmann, O. Yazyev, A. J. Austin, R. Cammi, C. Pomelli, J. W. Ochterski, R. L. Martin, K. Morokuma, V. G. Zakrzewski, G. A. Voth, P. Salvador, J. J. Dannenberg, S. Dapprich, A. D. Daniels, Ö. Farkas, J. B. Foresman, J. V. Ortiz, J. Cioslowski, D. J. Fox, Gaussian, Inc., Wallingford CT, **2009**.

[44] J. P. Perdew, K. Burke, M. Ernzerhof, *Phys. Rev. Lett.* **1996**, 77, 3865-3868.

[45] G. A. A. Saracino, R. Improta, V. Barone, *Chem. Phys. Lett.* **2003**, 373, 411-415.

[46] E. Runge, E. K. U. Gross, *Phys. Rev. Lett.* **1984**, 52, 997-1000.